

NAS5-28752

NASA Technical Memorandum 87808

**A Survey of Nested Grid
Techniques and Their Potential
for Use Within the MASS Weather
Prediction Model**

(NASA-TM-87808) A SURVEY OF NESTED GRID
TECHNIQUES AND THEIR POTENTIAL FOR USE
WITHIN THE MASS WEATHER PREDICTION MODEL
(NASA) 28 p

N87-18944

CSCI 04B

Unclas

G3/47 43632

**Steven E. Koch
Goddard Space Flight Center
Greenbelt, Maryland 20771**

**Jeffery T. McQueen
ST Systems Corporation
Hyattsville, Maryland 20784**



National Aeronautics
and Space Administration

Scientific and Technical
Information Branch

1987

NASA Technical Memorandum 87808

**A Survey of Nested Grid
Techniques and Their Potential
for Use Within the MASS Weather
Prediction Model**

Steven E. Koch and Jeffery T. McQueen

February 1987

INTRODUCTION

Nesting a fine mesh within a coarse mesh grid model is an economical way to improve the horizontal resolution in model forecasts of small-scale weather phenomena. Better resolution of intense horizontal gradients can be achieved without requiring a fine resolution grid throughout the whole model domain, thus saving computer time and memory space. Nesting effectively permits useful weather forecasts to be made for a longer period of integration than would otherwise be possible. Figure 1 shows an example of a nested grid mesh structure in both one and two dimensions (Kurihara et al., 1979). The ratio of gridbox size for the coarse mesh to that for the next finer mesh is always an integer—in this case, two. In this particular example, a triply nested system was used, where each mesh, except for the innermost one, enclosed a finer resolution mesh. A large number of researchers (Harrison, 1973; Elsberry and Ley, 1976; Jones, 1977a; Phillips, 1979; Kurihara and Bender, 1980) have used such multiply nested grids primarily to provide a more gradual change between grid meshes and to give smoother solutions near the boundary. Also, a gradual reduction can save substantial amounts of computer time and memory utilization since the finest mesh grid is reduced in size allowing a grid of intermediate resolution to serve as a buffer zone between the coarse and fine grid.

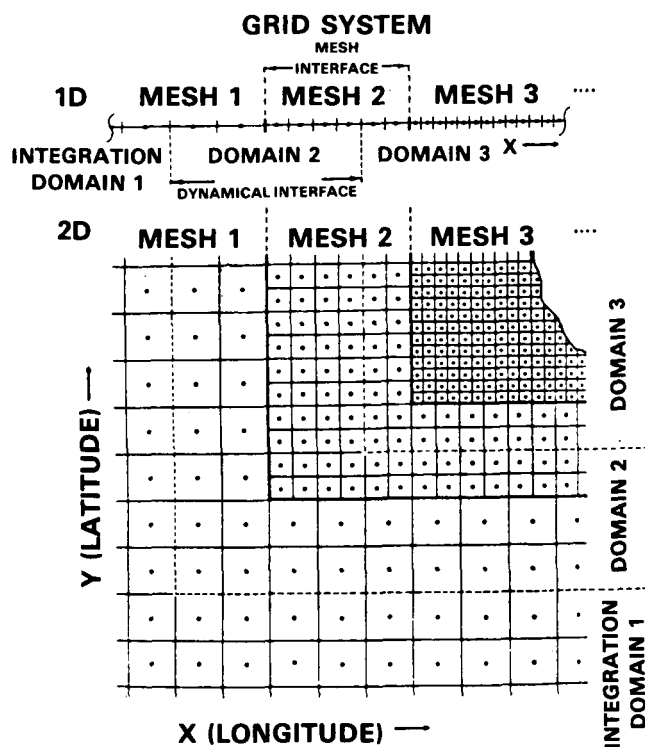


Figure 1. An example of nested grids (dots) in one-dimensional (upper part) and two-dimensional (lower part) domains (Kurihara, et al., 1979).

The interaction between the fine mesh grid and the larger scale model is performed through either one- or two-way interactive nesting. In the simpler one-way approach, waves can exit the coarse grid and enter and affect the fine mesh domain, but waves from the fine mesh cannot affect the coarse grid model since feedback from the fine grid is precluded. According to Elsberry and Ley (1976), the inherent assumption in this approach is that large-scale motions determine the small-scale motions without significant feedback from processes occurring within the fine mesh grid. In this case, the fine mesh and coarse mesh models usually run independently.

Two-way interacting schemes, which involve more programming effort, allow information from the coarse grid model to enter the fine mesh and perturbations from the fine mesh to exit into and affect the coarse mesh fields, since the predictions on both meshes proceed simultaneously. Grid interaction is accomplished with boundary conditions specified at the interface where the coarse mesh grid (CMG) and fine mesh grid (FMG) are coincident. Either values of the dependent variables or their time tendencies are interpolated in space and time to obtain FMG values from the CMG values near the interface. Simultaneously, the FMG affects the CMG forecast by replacing CMG values at the interface with ones (typically averaged) from surrounding FMG points.

The two-way interactive nested grid method is intuitively the more appealing of the two approaches' because the exchange of information between the two grids is more realistic, particularly when strong mesoscale disturbances are generated within the FMG (Phillips and Shukla, 1973; Anthes, 1983; Zhang, et al., 1986), although one-way schemes may actually give less noisy solutions (Sundstrom and Elvius, 1979). Tests which have been performed to examine the relative benefits of either method have employed either the advection, "shallow-water" wave, or lee wave equations (Harrison and Elsberry, 1972; Phillips and Shukla, 1973; Clark and Farley, 1984). Systematic comparative experiments conducted under more realistic atmospheric conditions, such as those encountered in sloping baroclinic zones with diabatic effects, have not yet appeared in the published literature, as far as we know. It is the purpose of this paper to review and contrast different techniques that have been developed to treat the lateral boundaries of one- and two-way nested grid models, and to suggest an experimental procedure for systematically evaluating the most promising of these nested grid techniques in a realistic baroclinic setting. The main emphasis of this survey is hydrostatic, limited-area models, although occasional reference to anelastic models, such as those used to simulate lee waves or deep convection, will be made where appropriate.

The general outline of this report is as follows. Relative advantages and disadvantages of one- and two-way nesting strategies are discussed beginning on page 2. Several of the most commonly used lateral boundary schemes

applicable to one-way nested gridding will be discussed beginning on page 5. Various two-way nested schemes are reviewed beginning on page 11. Next we discuss strategies for simultaneously initializing the fine and coarse meshes in one- and two-way nested grid models. Finally, recommendations for systematically evaluating the most appealing nested grid techniques using both adiabatic and diabatic versions of the Mesoscale Atmospheric Simulation System (MASS) numerical weather prediction model at NASA/GSFC (Kaplan, et al., 1982) are suggested.

ONE-WAY VS. TWO-WAY NESTING STRATEGIES

In principle, one-way nesting schemes are much simpler to encode than two-way nesting schemes and may be adequate in meteorological cases where the small-scale atmospheric phenomenon of interest does not impact significantly on its surrounding environment. An example of this type of weather event might be a sea-breeze type circulation where the feedback to the synoptic scale is minimal. Contrastingly, FMG boundary values are averaged and fed back to the CMG in a two-way nesting scheme. This helps the model predictions on each mesh to be more consistent with each other than would be possible with one-way nesting, and also allows the coarse grid mesh to respond to meteorological phenomena that can significantly impact their surroundings, such as hurricanes, mesoscale convective clusters, or squall lines. Although the two-way interaction approach is appealing from a physical point of view, one-way techniques may actually give smaller errors because waves leaving the FMG may generate fictitious gravity waves and other "noise" upon entering the CMG in a two-way scheme (Sundström and Elvius, 1979), as is discussed below.

Well-Posed Boundary Conditions

In order to better understand the kinds of errors that can be generated at the interface between the two different grid meshes, and why such errors are generated in the first place, it is necessary to consider what should be the proper formulation of boundary conditions for limited-area models. This critical question was addressed in an excellent survey article by Sunström and Elvius (1979). Fundamentally, the system of equations describing the fluid are "well-posed" if the initial and boundary values determine the solution uniquely for the entire period of integration and if small errors in these data produce errors of a comparable size in the solution. The non-hydrostatic form of the linearized Eulerian equations of motion are well-posed because boundary conditions can be properly formulated for this hyperbolic system of partial differential equations. A combination of (1) *specified* boundary values for the tangential velocities and potential temperature at the *inflow* boundary and (2) normal velocity and pressure determined from the *characteristics* of the system at *both* the inflow and outflow

produce a well-posed problem for this system in three space dimensions (Oliger and Sundström, 1978).

Unfortunately, the introduction of the hydrostatic approximation in the primitive equations, and, moreover, heat transfer and viscous processes in the atmospheric boundary layer, makes the Eulerian system no longer hyperbolic, except in the special case of the barotropic "shallow-water" equations. Therefore, it is no longer a straightforward matter to compute the characteristics within the FMG of a nested limited-area model utilizing the primitive equations (Sundström and Elvius, 1979). Most likely, it is for this reason that comparisons between one- and two-way interaction schemes have been made with hyperbolic systems of equations (Harrison and Elsberry, 1971; Phillips and Shukla, 1973; Clark and Farley, 1984). It is not obvious, therefore, that conclusions drawn from those experiments about the relative superiority of two-way schemes, can be automatically applied to more general atmospheric situations.

Sources of Boundary Condition Errors

Since no formulation of boundary conditions for the hydrostatic primitive equations can be well-posed, all nesting techniques will produce at least some error. This is true for both finite-difference and finite-element methods, although Raymond and Garder (1976) showed that use of a dissipative Galerkin procedure can greatly reduce the noise. The sources of these errors include everything from basic mathematical inconsistencies to the complicated manner in which the boundary conditions may be computed.

Errors are produced in two-way schemes due to the fact that different mesh sizes act like different propagation media to the waves, i.e., the slopes of the characteristics are affected (e.g., Phillips and Shukla, 1973; Sundström and Elvius, 1979). The size of this error source naturally depends upon the ratio of the grid sizes. These differences in phase velocity generate false waves of all kinds at the interface, which are reflected back into the FMG, perhaps to become trapped for a long time in the interior grid (Matsuno, 1966). In addition, some waves which are resolvable on the FMG but not the CMG may be aliased and suffer drastic amplitude reduction as they enter the CMG. These two error sources—characteristics alteration and change in resolution—affect only two-way interaction schemes. The small-scale noise near the interface and within the FMG is a combination of interference between waves crossing the interface from both grids, scattering of waves poorly resolved by the coarse grid, and reflection of waves entering the CMG back into the FMG. Jones (1977b) and others have found that wavelengths smaller than six coarse gridlengths are totally reflected and trapped within the FMG.

Errors in both one- and two-way interaction techniques are due to overspecifying the boundary conditions, resulting in erroneous wave reflections at the interface. By "overspecification" it is meant that more values are used from the coarse mesh than are actually required to extrapolate

(or "blend") those values to (with) the FMG values. Sundström and Elvius (1979) state the optimum boundary conditions for one-way schemes should have these properties:

- 1) "The boundary conditions should determine the major quasigeostrophic part of the solution accurately when the motion is inward. At outflow, this type of wave should pass through the boundary without any large reflection as computational modes or as gravity waves."
- 2) "Fast-moving gravity waves generated in the interior should pass through the boundary, if possible. At least they should not be reflected and amplified by the boundary conditions."

None of the one-way interaction schemes to be discussed in this report satisfy both of these conditions. Sundström and Elvius (1979) suggest that use of the following extrapolation formula on the outflow boundary satisfies these conditions, at least for the advection and shallow-water equations:

$$\phi_B^t = 2\phi_{B-1}^{t-1} - \phi_{B-2}^{t-2}, \quad (1)$$

where ϕ_B^t represents any prognostic variable at the boundary point B at time t. This equation describes the characteristics of these hyperbolic linear systems. Of course, it remains to be determined how effective this approach would be for non-hyperbolic systems, and whether the general principle of "specify at the inflow boundary, calculate the characteristics at the outflow boundary" applies to the hydrostatic primitive equations. Indeed, since the characteristics of these equation systems are not known, some kind of substitute method must be employed, such as extrapolation, calculation of some kind of "representative" wave phase velocity, or reliance upon more pragmatic, engineering strategies.

Baumhefner and Perkey (1982) defined two types of errors that occur at the interface between two different sized meshes: those that are generated by the boundary formulations, and those that are caused by incorrect data specification at the boundary. They concluded that both error sources contribute equally to the total error in one-way nested models. Boundary formulation errors arise from problems in "blending" the solutions from the two grids used in one-way nested models, and in defining the "interface conditions" used in two-way nested models (to be described in detail later in this paper). Boundary specification errors, on the other hand, are caused by using incorrect values in the specification of the boundary values, the result of errors in the forecast by the coarser mesh model near the fine grid model boundary. Pielke (1985) has shown that specification errors will introduce a fictitious acceleration throughout the entire model domain, the error being inversely proportional to domain size.

Pragmatic Determination of "Optimum" Boundary Conditions

The lack of purely mathematical principles to guide the

development of well-posed boundary conditions in hydrostatic limited-area models employing the diabatic, viscous primitive equations has motivated modelers to consider alternative philosophies for choosing "optimum" boundary conditions. For example, Zhang et al. (1986) suggest the optimal interface procedure for minimizing boundary formulation errors has the following properties: 1) all resolvable waves must propagate across the interface smoothly without generating significant noise, and 2) mass, momentum, and total energy exchanged between the two grids must be conserved. Typically, smooth wave passage is attainable only by employing some method of noise control. The following types of boundary conditions, described in detail beginning on page 5, have been used both as interface conditions and to control noise in one-way nesting systems.

- sponge boundary dampening and tendency blending schemes (Perkey and Kreitzberg, 1976; Miyakoda and Rosati, 1977)
- radiation schemes (Orlanski, 1976)
- flow relaxation schemes (Davies, 1976; Leslie, et al., 1981)
- extrapolation type schemes (Williamson and Brown-ing, 1974).

Jones (1977b) and Zhang et al. (1986) discuss four general ways to control noise in two-way systems:

- using smoothing operators (Jones, 1977a; Phillips, 1979)
- enhancing eddy diffusivities in the difference equations (Harrison and Elsberry, 1972; Elsberry and Ley, 1976; Kurihara and Bender, 1980; Zhang et al., 1986)
- modifying the interface condition to remove overspecification (Jones, 1977b)
- selecting a time integration damping scheme (Ookochi, 1972; Phillips, 1979; Kurihara, et al., 1979)
- employing a mesh separation scheme (Kurihara, et al., 1979; Phillips, 1979; Zhang, et al., 1986).

Some combination of these approaches is often used. For example, the mesh separation technique involves physically separating the boundary along which information from the CMG enters the FMG from that along which occurs the feedback of the FMG to the CMG (Kurihara et al., 1979; Phillips, 1979; Zhang, et al., 1986). This strategy separates the interface from the immediate impact of boundary formulation errors (p. 12ff), yet at least another noise control method must be used in conjunction with it.

The second optimal interface condition of mass, momentum, and energy conservation across the interface can be satisfied only if the *interpolation* formula used to derive boundary values for the FMG from the CMG is reversible as the *averaging* formula used to calculate the boundary points for the CMG from the FMG. This procedure has been used in a hydrostatic model by Kurihara et al. (1979) and in an

anelastic model by Clark and Farley (1984) to eliminate spurious mass accumulation at the boundary. The latter study found the conservative interface conditions to result in a dramatic reduction in errors, although such improvements may be peculiar to anelastic models. Zhang et al. (1986) sacrificed the conservation condition in a hydrostatic model for the sake of simply obtaining a smooth solution at the interface.

Comparison Tests Between One- And Two-Way Nesting Schemes

A limited number of tests using simple hyperbolic wave systems of equations have been performed thus far to study which nesting schemes may be superior. Caution must be exercised in attempting to generalize these results to hydrostatic models that utilize the fully viscous, diabatic primitive equations, as discussed earlier. In spite of this limitation, it is instructive to consider these studies and the general method of verification employed therein.

Harrison and Elsberry (1972) remarked that in an ideal nested grid system, the solution on the nested FMG part of the domain must exactly replicate that for a model which uses the FMG resolution everywhere. This verification technique for testing various nested grid strategies has been used by Harrison (1973) and Kurihara and Bender (1980). In practice, however, this type of verification is difficult to accomplish in three dimensions because of the large amount of grid points needed for the extended fine mesh control run. The most popular method of verification has been to analytically initialize the nested grid model and compare the forecast to the analytic solution. Harrison and Elsberry (1972) performed tests with a one-dimensional, linear, advection wave equation model, while Phillips and Shukla (1973) used a two-dimensional, hydrostatic, shallow water wave model to compare one- versus two-way nested grid schemes. More recently, Clark and Farley (1984) completed tests with a two-dimensional anelastic model of lee waves. Harrison and Elsberry (1972) found that the two-way interactive boundary conditions performed much better, in the sense that a much smoother solution than that given by the one-way nested model was obtained (Figure 2). They suggested that the interface noise in the one-way scheme would lead to aliasing and perhaps computational instability in a nonlinear model. However, no smoothing was utilized to control boundary formulation noise. Furthermore, the ratio of the time steps used in the two grids ($\Delta t_f/\Delta t_c$) was not equal to the ratio of the grid sizes ($\Delta x_f/\Delta x_c$), as it should be for consistency. Thus, their conclusions may not have truly general implications.

The Phillips and Shukla (1973) experiment showed a modest improvement in the solution when using the two-way nested grid model (Figure 3), particularly in the geostrophic part of the simulation. Clark and Farley's (1984) results from their anelastic lee wave simulations revealed a more dramatic

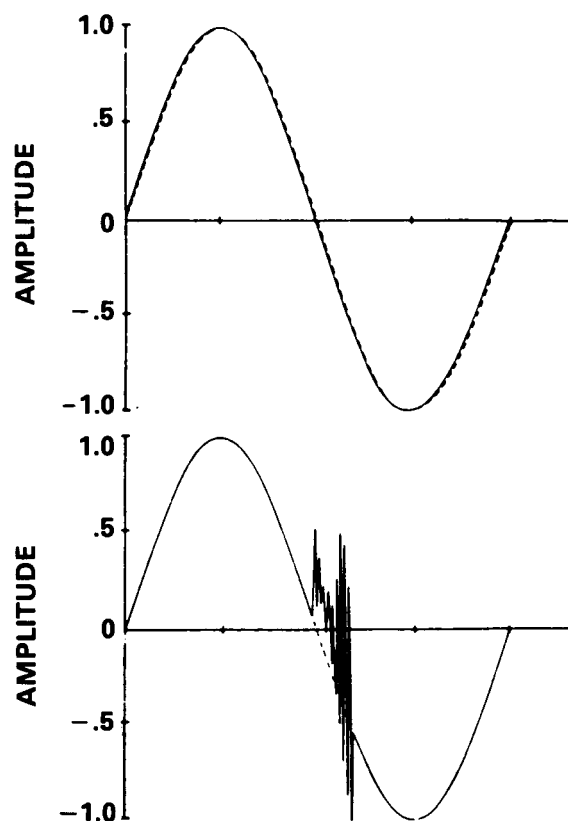


Figure 2. Numerical (solid) and exact (dashed) solutions after 4000 time steps of integration of the one-dimensional linear advection equation model of Harrison and Elsberry (1972). Two-way (one-way) interactive boundary conditions used in upper (lower) figure. Extent of CGM model domain equals wavelength of sinusoidal wave.

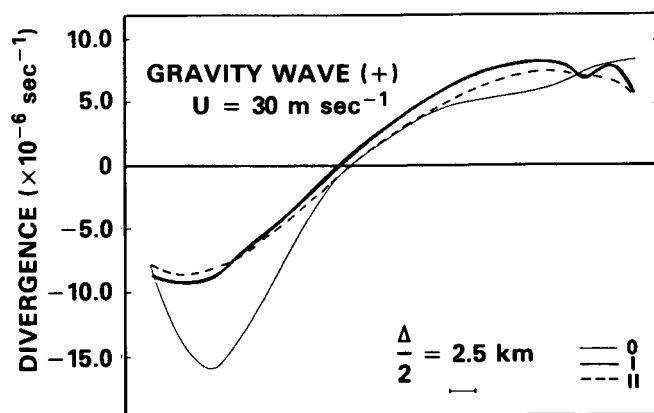


Figure 3. Distribution of horizontal divergence (10^{-6} s^{-1}) for the positive gravity wave simulations on a basic current used by Phillips and Shukla (1973). Case 0 is the analytic solution, case I is the solution with a one-way nested grid, and case II is that with a two-way nested grid. See Tables 4-6 for model details.

improvement in the two-way interactive system compared to the one-way nested grid model. Their FMG prediction at 4 hrs of vertical motion (w), perturbation potential temperature (θ'), and vertical vorticity component (η) using both kinds of nested grid systems are shown in Figure 4. Irregularities and

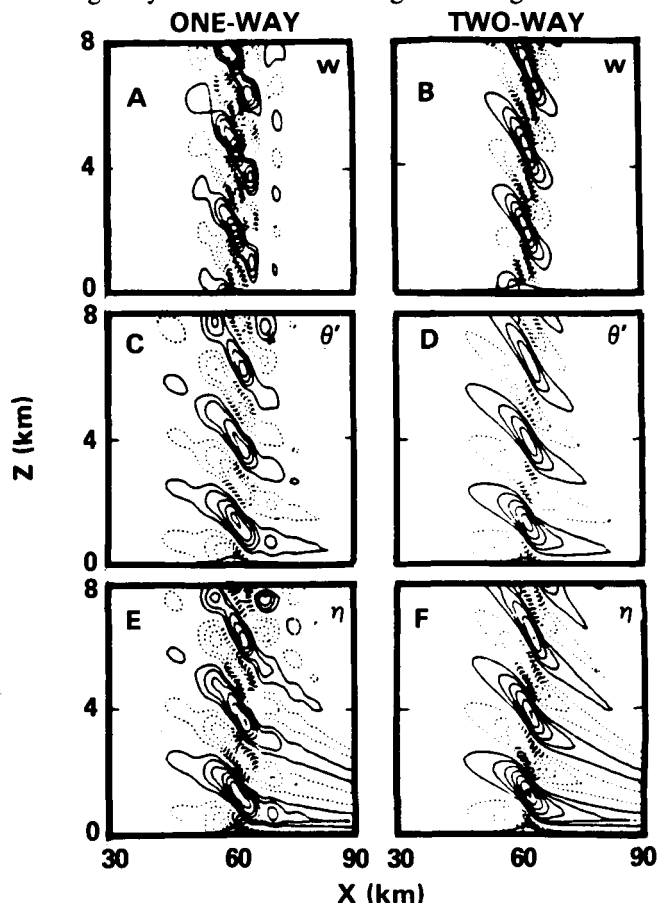


Figure 4. The time development of w , θ' , and η from the two-dimensional anelastic wave experiments of Clark and Farley (1984). Left (right) column shows results using a one-way (two-way) nested grid. Plates (a) and (b) show w after 4 hours with a contour interval of 0.05 m/s; (c) and (d) show θ' at the same time with a contour interval of 0.1K; (e) and (f) show η with a contour interval of $6 \times 10^{-4} \text{s}^{-1}$.

multiple local extremes found in the one-way simulations are the results of poor upper boundary conditions taken from the CMG. Comparing Phillips and Shukla's results, Clark and Farley ascribed their more significant improvement in two-way over one-way nesting systems to the elliptical nature of the anelastic system, although they did not elaborate upon their reasoning. Therefore, we do not know whether these results may apply to a hydrostatic nested grid framework.

In summary, it appears that no investigation thus far has convincingly demonstrated the clear superiority of two-way over one-way nesting schemes in hydrostatic primitive equation models. There is an even greater lack of demonstration

for numerical predictions of weather systems with real data initialization. Intuitively, one might expect an improved performance by allowing the two grids to interact with one another, but this needs to be demonstrated using both adiabatic and diabatic model predictions of a wide variety of atmospheric phenomena.

A SURVEY OF ONE-WAY INTERACTIVE SCHEMES

Four general types of one-way nesting strategies have been proposed and are reviewed here: sponge blending, flow relaxation, advective extrapolation, and radiation. Mixed combinations of these more general schemes are addressed also.

Sponge Blending

Sponge blending-type boundaries are pragmatic engineering approaches to incorporating the large-scale information from the coarse model into the fine grid. Formulation of this scheme involves modifying the boundary variable tendencies so that the coarse- and fine-grid tendencies are weighted or "blended" together in a zone near the boundary of the FMG. Enhanced filtering or diffusion is used near the boundary to dampen advecting wave disturbances as they approach the boundary zone. Consequently, reflection of spurious shorter wavelength noise back into the fine grid is minimized, while leaving the main solution unaltered. This type of scheme, first employed by Perkey and Kreitzberg (1976), has been used extensively in nested meteorological models.

Tendency blending is incorporated within a boundary zone of a one-dimensional model by using

$$\frac{\partial \hat{\phi}}{\partial t} \Big|_x = W(x) \frac{\partial \phi}{\partial t} \Big|_x + [(1-W(x))] \frac{\partial \Phi}{\partial t} \Big|_x \quad (2)$$

where Φ represents the specified coarse grid variable and $\hat{\phi}$ and ϕ denote the fine-grid model variable before and after blending, respectively. Values of the weighting coefficients, $W(x)$, used by several investigators are shown in Table 1. This shows that the tendencies for all the prognostic variables at the boundary point of the nested grid are totally specified by the coarse-grid model, whereas inward of this point, the tendencies are progressively weighted toward the fine-grid model forecasts.

The system is completed by employing some type of low-pass filter or increased diffusion near the boundary to act as a "sponge." Filtering or diffusion reduces the erroneous reflection of waves entering the boundary zone, thus giving the desired effect that the waves exit the fine grid model through the boundary with little alteration in form. The sponge also acts to reduce short-wave energy caused by the overspecification of the prognostic variables at the boundary.

TABLE 1. Weighting coefficients $W(x)$ used in blending. "B" represents the boundary grid point, B-1 the next FMG point inward of B, and so on. One-dimensional FMG domain size denoted by L.

Model Reference	Model Grid Point					
	B	B-1	B-2	B-3	B-4	B-5...B-L/2
Perkey and Kreitzberg (1976)	0.0	0.40	0.70	0.90	1.00	1.00
Baumhefner and Perkey (1982), NMC - LFM	0.0	0.40	0.70	0.90	1.00	1.00
Leslie, et al. (1981)*	0.0	0.33	0.67	1.00	1.00	1.00
	0.0	0.46	0.76	0.96	0.96	1.00

*This scheme is actually a flow relaxation type described later with the values shown being those of the relaxation coefficients.

Pielke (1985) warns, however, that the sponge should not be applied abruptly since erroneous reflection can result. Most of the filtering or diffusion forms used in the sponge-type schemes reviewed here appropriately used a gradually increasing smoother in a region near the boundary (Table 2). Perkey and Kreitzberg (1976) used a smoother-desmoother filtering function to remove the short-wave energy near the boundary in their primitive equation model runs, while a diffusion approach was employed in tests conducted with the advective wave equation (with similar results). Baumhefner

and Perkey (1982) gradually increased the horizontal diffusion coefficient to five times the normal value as the boundary was approached. Miyakoda and Rosati (1977) used both a filter (termed "boundary adjustment") and horizontal diffusion in their sponge version of a nested grid model. However, no blending of the large-scale tendencies was included. Instead, the large-scale variables were simply specified at the fine-grid boundary point. This approach was later shown to be unstable by Davies (1983), who also pointed out that significant wave reflection occurs when blending is not used.

TABLE 2. Description of filtering or diffusion used in the boundary zone for sponge-type one-way nested grid models. Φ_i represents any prognostic variable (at grid point i) "B" indicates the boundary grid points, while "I" refers to interior grid points. "K" is the diffusion coefficient. Δt_f and Δt_c are fine and coarse grid timesteps, respectively.

Authors	Nested Grid Model Type	Filtering Equation	Diffusive Operator		Frequency of Sponge Application
			Type	Boundary Application	
Baumhefner and Perkey (1982)	3-D Primitive equation	None	2nd order	B → B-2: $K_B = 5K_I$ B-3 → B-4: $K_B = 2K_I$	$2\Delta t_f$
Miyakoda and Rosati (1977)	3-D Primitive equation	$\hat{\phi}_i = \phi_i/2 + (\phi_{i-1} + \phi_{i+1})/4$, B-1 → B-3	---	B-1 → B-6: $K_B = 25K_I$	Δt_f
Perkey and Kreitzberg (1976)	1-D Advective wave equation	None	2nd order 4th order	B-1: $\beta = 0.2400$ B-2 → B-5: $\beta = 0.0600$ B-6: $\beta = 0.0325$ >B-6: $\beta = 0.0050$ where $\beta^{1/2} = 2K \Delta t / (\Delta x)^2$	I: $15\Delta t_f$ B: $5\Delta t_f$
Perkey and Kreitzberg (1976)	2-D Primitive equation	$\hat{\phi}_i = \phi_i + K_s(\phi_{i+1} - 2\phi_i + \phi_{i-1})$. $K_s = .25$ on smoothing step B-1 → B-6	---	None	I: $15\Delta t_f$ B: $5\Delta t_f$

Moreover, since Miyadkoda and Rosati did not gradually increase the viscosity near the boundary (Table 2), an additional source of spurious wave reflection at the interface existed. In fact, they found that significant noise was generated when only a horizontal diffusion scheme with no filter was used. This is the reason why they found that a filtering function was also needed to obtain satisfactory results. It is likely that much of the noise could have been reduced had the diffusion coefficient been increased gradually and tendency blending been used.

A linear stability analysis must be performed when using a diffusion-type damping scheme. Perkey and Kreitzberg (1976) incorporated a diffusion scheme into a set of experiments that employed a simple one-dimensional advective wave equation. The accompanying stability analysis showed that the following criterion needed to be satisfied to maintain linear stability at all points greater than one FMG grid distance in from the boundary:

$$K \leq \frac{1}{16} \frac{(\Delta x)^2}{2\Delta t} \quad (3)$$

where K is a diffusion coefficient, Δt is the model timestep, and Δx represents the grid spacing. This result was obtained for a fourth-order diffusive filter, which was used near all boundary points, except for the point adjacent to the boundary (B-1) where second-order diffusion was used.

Baumhefner and Perkey (1982) and Miyakoda and Rosati (1977) both experimented with the magnitude of the diffusion coefficient near the boundary. Their results showed that when the diffusion was enhanced too strongly, boundary formulation errors also increased. The increased loss of large-scale wave information entering the fine-grid domain (caused by overdampening) was blamed for the errors. On the other hand, when the diffusion was too weak, considerable small-scale noise was generated at the interface. Baumhefner and Perkey (1982) concluded that the final choice of diffusive operator in sponge blending schemes must be made very carefully. Thus, a low-pass filter, where only shorter waves are damped out while longer wave features remain, could perhaps be better suited than a diffusion scheme.

Baumhefner and Perkey (1982) have also pointed out that *for diffusion to be effective, blending must be done before the diffusion sponge is applied*. This was shown by first writing the tendency equation for a one-dimensional diffusion (FMG) model as

$$\left. \frac{\partial \phi}{\partial t} \right|_x = [K(x)] \left. \frac{\partial^2 \phi}{\partial x^2} \right|_x \quad (4)$$

and then applying the blending equation (2) to yield

$$\left. \frac{\partial \phi}{\partial t} \right|_x = W(x)K(x) \left. \frac{\partial^2 \phi}{\partial x^2} \right|_x + [(1-W(x))] \left. \frac{\partial \phi}{\partial t} \right|_x \quad (5)$$

This shows that when blending is done on a tendency that has already been subjected to diffusion, the effect of diffusion is reduced by the weighting term. Comparison of model results in Table 2 does not indicate any agreement, however, as to how frequently to apply the sponge once the variable tendencies have been blended.

Experiments have been performed by some of these workers to determine the optimal frequency for blending (updating the boundary values of) the nested and coarse grid tendencies. Table 3 summarizes the various frequencies at which the boundary values have been updated in the past and gives details on the models used in these experiments. The basic rule is that the boundary must be updated frequently enough so that wave aliasing does not occur and that waves entering the FMG from the coarser grid model are properly resolved. This guideline would suggest that boundary values must be updated at least once every coarse-grid timestep. In one extreme case where Perkey and Kreitzberg (1976) used an update frequency of 45 coarse-grid time steps, a strong decrease in incoming wave amplitude resulted. This problem, of course, is one to be avoided by any boundary condition scheme used, not only sponge schemes.

Most of the investigators cited in Table 3 have found the sponge blending scheme to be stable in that errors did not grow rapidly during a model run. This scheme has also been found to be simple to program and easy to use. The reflection of spurious waves back into the center of the FMG domain is never completely eliminated, although it can be considerably diminished by using an appropriate sponge. Two pragmatic considerations have also been given by both Baumhefner and Perkey (1982) and Pielke (1985), who recommend: (1) enlarging the nested-grid model domain as far as possible past the area of interest to delay any contamination from the boundary, and (2) extending the boundary away from areas of strong activity to avoid errors caused by rapidly changing fields in the CMG, i.e., large-tendency values.

Flow Relaxation

This type of scheme, which was first developed by Davies (1976), is similar to the sponge type condition, in that prognostic variables in a zone near the boundary are forced to relax toward the large-scale data fields. However a relaxation coefficient is used instead of a smoother in the blending formulation and the prognostic equation for a variable ϕ is written in terms of a modified advection equation as

$$\frac{\partial \phi}{\partial t} = -U \frac{\partial \phi}{\partial x} - r(x) (\phi - \Phi) \quad (6)$$

where $r(x)$ is the relaxation coefficient and Φ is the externally specified value of ϕ at the boundary. The relaxation coefficient is gradually decreased toward the boundary so that the effect is not felt abruptly. A diffusion term like the one used in some of the sponge conditions may also be added to this equation.

TABLE 3. Model type, grid spacing, timesteps, and boundary data update frequency used in various one-way nested grid systems employing the primitive equations.

Authors	Model Type		Fine Grid		Coarse Grid		$\frac{\Delta x_c}{\Delta x_f}$	Frequency of Boundary Data Update
	Fine	Coarse	Δx (km)	Δt (min)	Δx (km)	Δt (min)		
Perkey and Kreitzberg (1976)	2-D	2-D	<u>Sponge - Type Boundaries</u>				2/1	$5\Delta t_f$
			60	2	120	4		
Miyakoda and Rosati (1977)	3-D Barotropic	3-D Hemispheric	135	2.5	540	10	4/1	Δt_c
Baumhefner and Perkey (1982)	3-D	3-D Hemispheric	~ 275	2.5	~ 550	5	2/1	Δt_c
Kaplan, et al. (1983)	3-D	3-D (LFM)	14	0.25	58	1	4/1	$60\Delta t_c$
Leslie, Mills, and Gauntlett (1981)	3-D	3-D Hemispheric	<u>Flow Relaxation Type Boundaries</u>				2/1	---
			125	18	250	36		
Williamson and Browning (1974)	3-D	3-D Global Circulation	<u>Extrapolation Type Boundaries</u>				4/1 to 2/1	Δt_c
			$\sim 69-275$	---	$\sim 138-550$	---		
Miyakoda and Rosati (1977)	3-D Barotropic	3-D Hemispheric	135	2.5	540	10	4/1	Δt_f

To solve (6) for ϕ^{t+1} , Leslie et al. (1981) suggest first estimating its value (ϕ_e^{t+1}) by solving the prognostic equation for ϕ^{t+1} with the boundary relaxation term excluded. The final solution for ϕ^{t+1} is found by time weighting as follows:

$$\phi^{t+1} = (1-\alpha)\phi_e^{t+1} + \alpha\phi^t, \quad (7)$$

where α is calculated in terms of r as

$$\alpha = 2r\Delta t / (1 + 2r\Delta t). \quad (8)$$

The nested grid system used by Leslie et al. (1981) is summarized in Table 3. The values of the relaxation coefficients are given in Table 1.

The boundary relaxation scheme can only be used where the predicted winds at the boundary are directed into the

model. On the outflow boundary, another scheme (such as the radiative scheme) must be used. Boundary conditions that depend on the wind direction at the boundary will be inherently troublesome when the wind is nearly parallel to the boundary or when there is both inflow and outflow on a boundary. Although Davies (1983) found this scheme to be stable, the scheme has not been thoroughly tested for more general situations such as those encountered with parallel flow at the boundary.

Advective Extrapolation

This type of boundary condition, described and used by Williamson and Browning (1974), determines the prognostic variables by one of two methods depending on the wind direction at the interface boundary. When the CMG winds are

directed into the FMG domain, the fine-grid prognostic variables at the boundary are *specified* from the CMG by a simple linear interpolation in space and time. When the coarse-mesh winds are directed out of the fine-grid domain, the boundary variables are *extrapolated* from the fine-grid interior to the boundary. This is simply obtained by horizontal advection by the *large-scale* wind. Horizontal diffusion is also increased at the closest two boundary points by a factor of four and at the next two interior points by a factor of two. The Williamson-Browning numerical model is summarized in Table 3.

This scheme, like flow relaxation schemes, relies upon the wind direction at the boundary in order to know whether to specify or extrapolate values. The boundary update occurs only at the boundary, providing no transition zone. Baumhefner and Perkey (1982) compared this scheme to the sponge blending condition and found the Williamson-Browning technique to be unstable, especially when the fine-grid spacing was much less than the coarse-grid spacing. Miller and Thorpe (1981) also found this extrapolation scheme to be unstable. Because of these problems, this boundary condition scheme will not be tested in the MASS model.

Radiation

This technique attempts to minimize the reflection of outward propagating waves back into the model domain by allowing them to radiate freely outward through the boundary. The radiation scheme is implemented in the east-west direction, for example, with a Sommerfeld (1964)-type wave equation of the form

$$\frac{\partial \phi}{\partial t} = -C_{\phi} \frac{\partial \phi}{\partial x} \quad (9)$$

Here ϕ is any prognostic variable and C_{ϕ} is the empirically-derived "typical phase velocity" for each variable, rather than an advection velocity as used in the previous two schemes. Orlanski (1976) introduced this approach by first solving for C_{ϕ} using a centered-centered finite difference approximation

$$C_{\phi} = - \frac{2 (\phi_{B-1}^t - \phi_{B-1}^{t-2})}{(\phi_{B-1}^t + \phi_{B-1}^{t-2} - 2\phi_{B-2}^{t-1})} \left(\frac{\Delta x}{2\Delta t} \right), \quad (10)$$

where B is the boundary grid point, B-1 is the next FMG grid point in from the boundary, etc., and C_{ϕ} is calculated for every prognostic variable under the limits that if $C_{\phi} \geq \Delta x/\Delta t$, it is set to $\Delta x/\Delta t$, whereas if $C_{\phi} < 0$ it is set to zero. Next, Orlanski reintroduced (9) in centered difference form, but now solved for ϕ at the next time step to update the boundary variables:

$$\begin{aligned} \phi_B^{t+1} &= \frac{[1 - (\Delta t/\Delta x) C_{\phi}]}{[1 + (\Delta t/\Delta x) C_{\phi}]} \phi_B^{t-1} + \\ &2 \frac{(\Delta t/\Delta x) C_{\phi}}{[1 + (\Delta t/\Delta x) C_{\phi}]} \phi_{B-1}^t. \end{aligned} \quad (11a)$$

The radiation condition is used to extrapolate waves only on boundaries where waves are propagating outward. Variable tendencies still have to be specified on an inflow boundary. The direction of wave movement is found from the phase velocity: if $C_{\phi} < 0$, an inflow boundary is defined, whereas if $C_{\phi} > 0$, an outflow is defined. Note that the extrapolation technique discussed earlier is a simplification of (11a) resulting from setting $C_{\phi} = \Delta x/\Delta t$, which yields

$$\phi_B^{t+1} = \phi_{B-1}^t \quad (11b)$$

Because the use of centered differencing near the boundary is inappropriate, Miller and Thorpe (1981) suggested an improvement to the Orlanski scheme. They used a forward upstream finite difference form of the equations for ϕ and C_{ϕ} , so that (11a) becomes

$$\phi_B^{t+1} = \phi_B^t - \tilde{r} (\phi_B^t - \phi_{B-1}^t), \quad (12)$$

where $\tilde{r} = C_{\phi} \Delta t/\Delta x$. The most accurate form of \tilde{r} , in terms of truncation errors, was found to be a combination of different forward upstream equations for r ,

$$\tilde{r} = \hat{r}_{u1} + \hat{r}_{u2} - \hat{r}_u, \quad (13)$$

where

$$\hat{r}_u = (\phi_{B-1}^t - \phi_{B-1}^{t-1}) / (\phi_{B-2}^{t-1} - \phi_{B-1}^{t-1}), \quad (14)$$

$$\hat{r}_{u1} = (\phi_{B-1}^{t+1} - \phi_{B-1}^t) / (\phi_{B-2}^t - \phi_{B-1}^t), \quad (15)$$

and

$$\hat{r}_{u2} = (\phi_B^t - \phi_B^{t-1}) / (\phi_{B-1}^{t-1} - \phi_B^{t-1}). \quad (16)$$

Here \hat{r}_{u1} and \hat{r}_{u2} are modifications to the time and space levels used in the usual form of the forward upstream equation for \hat{r}_u . A Taylor expansion performed on the truncation error showed that this form of the finite difference approximation to the radiation condition was third-order accurate, whereas the Orlanski form was only second-order accurate.

The radiation scheme studies of Orlanski (1976) and Miller and Thorpe (1981) are based on theoretical analyses, but not on the characteristics of the equations. Therefore, as Sundstrom and Elvius (1979) remarked, the solution will be polluted with errors if it is dominated by more than one wave mode, which, of course, naturally occurs in primitive equation models. Miyakoda and Rosati (1977) attempted to

extend the Orlanski scheme by applying it as an interface condition within a primitive equation model (Table 3). The radiation condition was applied at the outflow boundary once per fine-grid time step. On the inflow boundary, the coarse-grid model variables were interpolated in time to every fine-grid time step and then spatially interpolated to the boundary. Neither blending nor enhanced diffusion was used at the inflow boundary. However, the simple 1-2-1 filter was applied at all lateral boundaries, just as was done in the sponge experiments. Test results indicated that this radiation scheme reduced, but not entirely eliminated, wave reflection at the interface compared with their sponge scheme (panels RAD and AVIS, respectively, in Figure 5). The sponge results are,

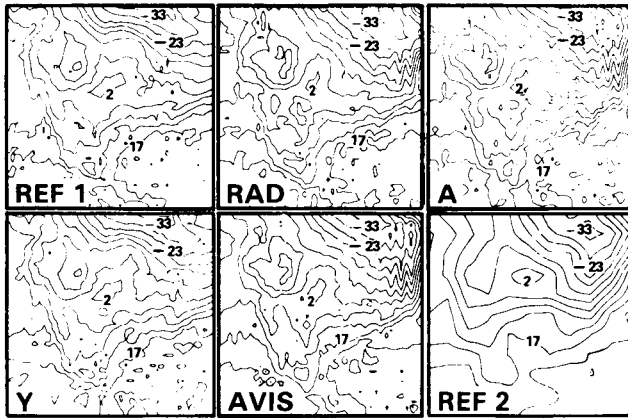


Figure 5. Temperature at 811 mb (contour interval 5° C) after 48 hours of integration of a three-dimensional barotropic model. From Miyakoda and Rosati (1977). REF1 refers to the fine grid hemispheric model and REF2, the coarse grid hemispheric model. The other four plates show results with one-way nested grid boundary conditions: (RAD) test using the radiation scheme and boundary adjustment; (A) test using REF2 data for FMG boundary values, Asselin filter, and boundary and hydrostatic adjustments; (Y) same as (A) except use of REF1 values for direct replacement at FMG boundaries; (AVIS) test of sponge scheme which employs both boundary adjustment and enhanced viscosity. Both RAD and AVIS used REF2 model data with no blending for the boundary conditions. See tables 2 and 3 for model details.

with the exception of one boundary, overly smoothed because of the harsh viscosity effect used by Miyakoda and Rosati (1977) in their sponge scheme (compare plates AVIS and A). They found the Euler-backward time marching scheme (used also in the MASS model) difficult to use with the radiation scheme tested; therefore, they switched to a leap frog time scheme with use of a time filter (Asselin, 1972). They also noted that their results were noisy when hydrostatic

equilibrium was not maintained along boundaries located over detailed mountainous terrain. A hydrostatic correction to the surface pressure, P_s , was calculated according to

$$\hat{P}_s = P_s [1 + (g/RT_v)(\hat{Z}^* - Z^*)], \quad (17)$$

where \hat{Z}^* is the interpolated topographic height obtained from the coarse-mesh terrain. The Asselin time filter and hydrostatic adjustment were included in experiments A, Y, RAD, and AVIS in Figure 5.

Davies (1983) cautioned that the utility of radiative boundary schemes is doubtful whenever diabatic heating or strong orography are in the vicinity of the boundary. These effects cannot be expected to be treated well since the phase velocity for only one portion of the wave spectrum is being calculated by (9), and the Sommerfeld problem only provides for an asymptotic solution far from the energy source for waves. Thus, boundaries should be kept away from areas of strong latent heat release and mountains where practicable.

Mixed Schemes and MASS Model Applications

Carpenter (1982) proposed a radiation scheme for use in nested-grid models that would blend the fine- and coarse-mesh variable tendencies at the interface. He obtained a generalized radiation boundary condition by applying (9) to both grids and assuming no inwardly propagating modes. This resulting equation,

$$\frac{\partial \phi}{\partial t} = \frac{\partial \Phi}{\partial t} - C_{\phi} \left(\frac{\partial \phi}{\partial x} - \frac{\partial \Phi}{\partial x} \right), \quad (18)$$

can be solved by using forward upstream finite differencing as suggested by Miller and Thorpe (1981). However, it is important to note that the derivation of (3.17) assumes that the phase velocities for both the coarse- and fine-mesh grids are equal, yet this is incorrect according to Olinger and Sundstrom (1978). It can easily be shown that the following equation results when this assumption is not made.

$$\frac{\partial \phi}{\partial t} = \frac{\partial \Phi}{\partial t} - C_{\phi} \frac{\partial \phi}{\partial x} - C_{\Phi} \frac{\partial \Phi}{\partial x}, \quad (19)$$

Unfortunately, Carpenter's proposals have not yet been tested in a nested grid model. Furthermore, solving the finite difference form of the wave equation on a nonstaggered grid may create additional interpolation error and noise (Miyakoda and Rosati, 1977). This is also relevant since the current version of MASS uses a nonstaggered grid.

Because of the limited use of radiation conditions in nested-grid models and the fact that Carpenter's generalization has never been evaluated, the success of such a scheme in a mesoscale model is uncertain. Furthermore, since variables must be stored from the previous two time steps [see (12)-(16)], the radiation condition requires somewhat more computer space and time allocations than the sponge schemes. Despite these drawbacks, the successful use of the

radiation condition by Miyakoda and Rosati (1977) and positive evaluation of it from a theoretical perspective warrants testing of Carpenter's (1982) scheme with the MASS model. The only other one-way nesting schemes with potential for use in a mesoscale model seem to be the sponge blending strategy developed by Perkey and Kreitzberg (1976) and, perhaps, the untested flow relaxation scheme of Davies (1983).

It should be noted that none of these schemes attempt to maintain any kind of dynamical or hydrostatic balance at the nested grid interface. Clearly hydrostatic imbalances are likely to develop because of the separate handling of the pressure, temperature, and velocity fields by the schemes. Miyakoda and Rosati (1977) have presented an approach for restoring hydrostatic equilibrium when it has been upset by the presence of mountains along the interface. This technique for adjusting the surface pressure, as well as other procedures for maintaining hydrostatic equilibrium and preventing the formation of superadiabatic lapse rates above the surface layer, must be considered when performing the MASS model experiments.

TWO-WAY INTERACTIVE NESTING TECHNIQUES

In this section, strategies used in two-way interactive nested grid models are reviewed. In particular, mesh structures, interface conditions, noise control techniques, time marching procedures, and general model characteristics are discussed. Table 4 presents some aspects of the two-way strategies found in our literature review, and Table 5 describes general characteristics of the nested grid models. These tables will be referred to frequently later in this section. The entries in these tables are similar to those in Table 1 of Zhang, et al. (1986), with these exceptions:

- Our tables include additional entries for interpolation type, mesh structure, grid ratios, form of finite difference equations, statistics regarding the model spatial and temporal differencing, and consideration of diabatic effects.
- More specific descriptions of methods used for interface conditions and noise control appear in our tables.

TABLE 4. Summary of two-way nesting techniques used in various models

Model Reference	Interface Condition for FMG	Type of Interpolation	Interface Condition for CMG	Mesh Structure	Ratio & (No.) of Grids	Conservation	Noise Control at the Interface
Birchfield (1960)	Variable interpolation	Linear	Value replacement from FMG at common points	Adjacent	2:1 or 4:1(N=2)	No	---
Ookochi (1972)	Weighted mean variable interpolation	Linear	Weighted mean averaging	Adjacent	2:1(N=2)	No	---
Harrison (1973, 1981), Harrison & Elsberry (1972)	Tendency interpolation	Cubic Lagrange	25 point area averaging (in 3-D)	Adjacent	5:1(N=2 or 3)	No	Laplacian diffusion everywhere + Euler-backward periodically
Phillips and Shukla (1973)	Variable interpolation	Polynomial	Interpolation of staggered FMG values	Separated by $2 \Delta x_c$	2:1(N=2)	No	---
Mathur (1974)	Variable interpolation	Cubic Lagrange	9 point averaging	Adjacent	2:1(N=2)	No	Laplacian diffusion everywhere
Elsberry & Ley (1976), Ley & Elsberry (1976)	Tendency interpolation	Cubic Lagrange	9 point averaging	Adjacent	2:1(N=3)	No	Laplacian diffusion everywhere + Euler-backward periodically
Jones (1977a,b)	Tendency interpolation	Cubic Lagrange	9 point Shuman filtering	Overlap	3:1(N=3)	No	Interfacial smoothing + upstream differencing on outflow interface
Phillips (1979)	Variable interpolation	Bilinear	Interpolation of staggered FMG values	Separated by $3.5 \Delta x_c$	2:1(N=3)	No	Smoother every 3 hrs. on FMG
Kurihara, et al. (1979), Kurihara & Bender (1980)	Variable interpolation	Linear conservative	Modified "Box" method	Separated by $2 \Delta x_c$	3:1 or 2:1(N=3)	Yes	Laplacian diffusion on FMG + "Box" method periodically
Zhang, et al. (1986)	Tendency interpolation	Lagrangian + cubic spline	9 point Shapiro filtering	Separated by $2 \Delta x_c$	3:1(N=2)	No	Laplacian diffusion everywhere + implicit Newtonian damping

TABLE 5. General characteristics of numerics and physics in various two-way nested grid models

Model Reference	Model Type	Form of Finite Difference Eqns.	Time Difference Scheme	Space Difference Scheme	Staggered Arrays	Fine Grid Vertical Levels	Δx_f (km)	Δt_f (sec)	Terrain	Diabatic Effect
Birchfield (1960)	Nondivergent barotropic	Advective	Leapfrog	Centered	No	1	150	900	No	None
Ookochi (1972)	Shallow water wave	Flux	Euler-backward	Arakawa Jacobian	Yes	1	300	600	No	None
Harrison (1973, 1981), Harrison & Elsberry (1972)	2-D & 3-D P.E.	Flux	Leapfrog	Centered	No	4	83 (40)	36 (?)	No	Analytic convective heating
Phillips and Shukla (1973)	Shallow water wave	Advective	Lax-Wendroff	Centered	Yes	1	25	270	No	None
Mathur (1974)	3-D P.E.	Advective	Quasi-Lagrangian advective	---	No	4	37	90	No	Cumulus param
Elsberry & Ley (1976), Ley & Elsberry (1976)	2-D & 3-D P.E.	Flux	Leapfrog	Arakawa Jacobian	No	4	51	120	No	Analytic convective heating
Jones (1977a,b)	3-D P.E.	Flux	Euler-backward	Centered	Yes	3-7	10	15	No	Cumulus param
Phillips (1979)	3-D P.E.	Flux	Lax-Wendroff	Centered	Yes	10	99	--	Yes	Cumulus param + large-scale precip
Kurihara, et al. (1979), Kurihara & Bender (1980)	1-D & 3-D P.E.	Flux	Modified Euler backward	Modified "box" method	No	23	18 (dry) 6 (moist)	30 7	No	Moist convective adjustment
Zhang, et al. (1986)	3-D P.E.	Flux	Brown-Campana	Arakawa Jacobian	Yes	19	40	~80	Yes	Cumulus param

Mesh Structure and Time Marching Procedures

The choice of mesh structure will determine to some degree how much noise will be generated at the interface boundary and also the complexity of the nested-grid code. Two types of mesh structures have been used extensively, with the single exception of Jones' (1977a,b) scheme discussed below (Table 4). These will be called the "adjacent" and the "separated" mesh structure in this review.

The adjacent mesh structure is the simplest and, prior to the last decade, the one most commonly used (Birchfield, 1960; Ookochi, 1972; Harrison and Elsberry, 1972; Harrison 1973, 1981; Mathur, 1974; Ley and Elsberry, 1976). Figure 6 gives an example of this type of mesh from the triply nested model of Harrison (1973). Boundary values are specified at each of the two-way interactive mesh interfaces. Time marching for this type of grid structure proceeds from the coarsest to the finest and back again, as described in Figure 7. The CMG is integrated one time step (points A to E), the MMG (medium mesh grid) boundaries are updated from spatial and temporal interpolation of the MMG-CMG interface values, and the MMG is then integrated one MMG time step (points A to C). For this case, two time steps are taken in the FMG to raise the solution to the MMG timestep (point C). The FMG boundary values are supplied through

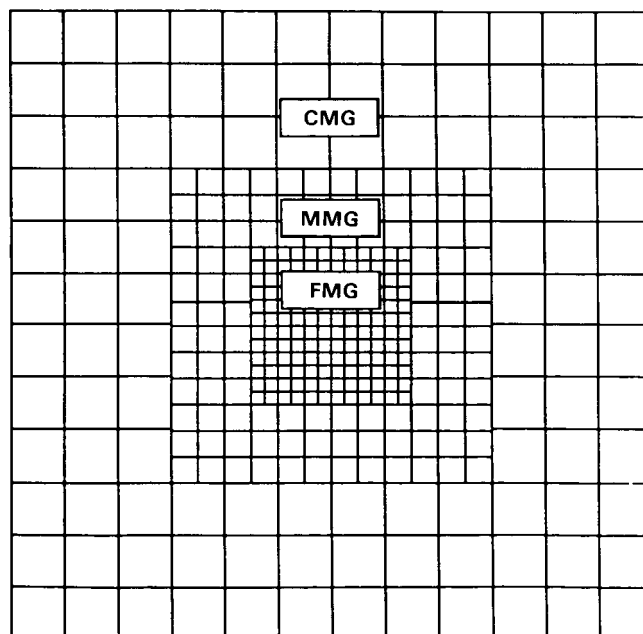


Figure 6. Example of a horizontal level in a triply nested grid model using an adjacent grid mesh structure. For this example, each of the smaller grids uses one-half the spatial increment of the next larger (Harrison, 1973).

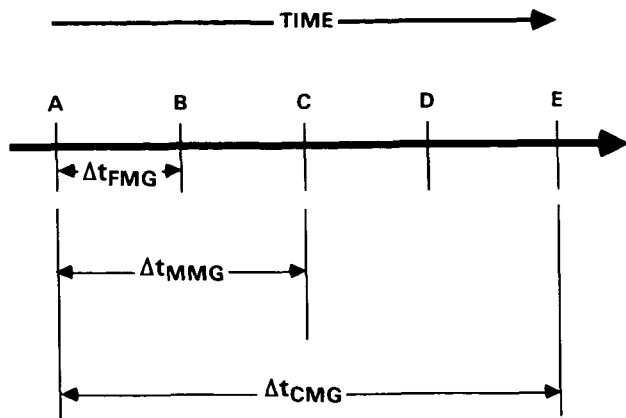


Figure 7. Schematic to indicate the time marching process in a two-way, triply nested grid model. The heavy line indicates any arbitrary position in time after the first time step, with the time between each point on the line representing one FMG time increment (Harrison, 1973).

interpolation from its interface with the MMG. Finally, the finer grids are raised to the coarse grid time by repeating the above technique from points C to E. The two-way interaction is completed when the CMG internal boundary values are calculated by averaging surrounding MMG points. Thus, the forcing by the CMG and the feedback from the MMG to the CMG both occur at the same interface (similarly for the MMG-FMG two-way interaction).

While the adjacent mesh structure is simple, it suffers from the fact that the interpolated values for the boundaries of the FMG are obtained from values on the surrounding coarser grid which have themselves been averaged or interpolated from previously forecast FMG values. Such interpolation between values which had themselves been interpolated presents an overspecification problem at the boundaries, and numerical errors can result at the interface. One way to avoid these problems is to use a grid mesh structure which separates the CMG→FMG input interface from the FMG→CMG feedback interface (Phillips and Shukla, 1973; Phillips, 1979; Kurihara, et al., 1979; Kurihara and Bender, 1980; Zhang et al., 1986), an example of which is shown in Figure 8. This particular scheme uses a $2\Delta x_c$ separation interval. Notice that the CMG internal boundary ("feedback" or "mesh" interface) and FMG external boundary ("input" or "dynamical" interface) are separated. In some applications, the FMG is actually extended to the input interface, thereby overlapping the CMG by a few grid points. This is done to simplify the interpolation or averaging done at the feedback interface. Either interpolated variables or their tendencies provide boundary conditions for the FMG at the input interface, whereas the FMG fields are either interpolated or smoothed to provide CMG field values for coincident points at the feedback interface (Table 4). This approach of

separating the two interfaces ensures that only internally forecast FMG values are used for the feedback calculations. The result is a desirable reduction in the level of quasi-stationary short-wave noise which would otherwise appear on both grids as the result of overspecification when using a single interface (Zhang, et al., 1986).

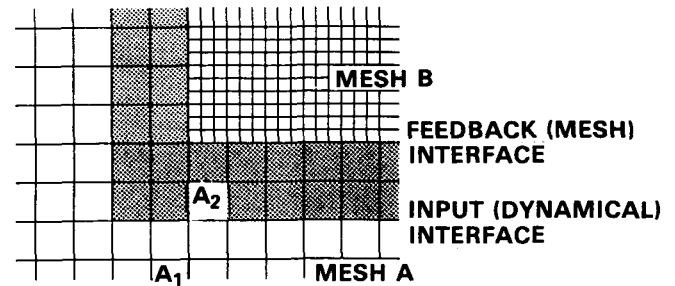


Figure 8. Separation of the input (dynamical) interface from the feedback (mesh) interface by a narrow zone A2 (shaded) in a two-dimensional domain. Area A1 is the coarse mesh. From Kurihara and Bender (1980). Terms "input" and "feedback" are used by Zhang, et al. (1986) and in the present review.

The time marching procedure for the interface separation approach proceeds as follows (Figure 8). In the first step, the prediction is made using the CMG timestep for the coarse grid area A1 by using data in both areas A1 and A2 (outside the feedback interface). In the second step, the forecast values at the input interface are saved and used as boundary conditions for integrating over both the CMG within area A2 and the FMG within area B, but using the FMG time step for both domains. Hence, some type of time interpolation to the FMG time must be performed at the input interface boundary. This is done for a few time steps until the FMG time is updated to the CMG time (as in Figure 7). In other words, the input interface represents a change in temporal resolution, whereas the feedback interface defines the boundary separating a change in spatial resolution (Clark and Farley, 1984). This scheme is two-way interactive since the area outside the input interface is influenced by inner area A2 in step 1 and the inner area is affected by the outer CMG area in step 2.

The mesh structure used by Jones (1977a,b) differs from all the above schemes in that the CMG is extended throughout the entire FMG domain. This use of grid overlays results in feedback from the FMG to the CMG at all coincident points within the FMG, not just at an interface or within a narrow zone of mesh separation. The FMG→CMG feedback is then accomplished through application of a 9-point smoother to the FMG data surrounding the CMG points. Despite use of this filter, noise grew throughout the interior of the FMG, which necessitated application of an additional filter near the

interface at alternate time steps. This was not surprising, considering that CMG values within the FMG domain were continually updated at the feedback step, yet no input to the FMG was provided by the CMG data in the interior of the FMG domain.

Interface Conditions

Interface conditions typically involve interpolating CMG variables or tendencies to obtain the boundary conditions for the FMG, and smoothing (averaging) FMG variables or tendencies to specify the interface conditions for the CMG (Table 4). Some modelers have sought to obtain an interface condition that conserves mass, momentum, and energy by requiring that the interpolation formula used to derive the FMG boundary condition be consistent with the averaging equation used to obtain the CMG boundary condition. Stated another way, the CMG→FMG interpolation formula and the FMG→CMG averaging process should be reversible. Therefore, the averaging and interpolation formulas applied to any variable ϕ should be, respectively, of the form (Clark and Farley, 1984)

$$\Phi = \left(\frac{\Delta x_f}{\Delta x_c} \right) \sum_{i=1}^n \phi_i, \quad (20a)$$

and

$$(\Delta x_f) \sum_{i=1}^n \phi_i = (\Delta x_c) \Phi. \quad (20b)$$

Where n is the integer ratio, Δx_f is the FMG grid size, Δx_c is the CMG grid size, and ϕ and Φ can represent either prognostic variables or their tendencies over the FMG and CMG, respectively. These two linear equations ensure that mass continuity is not destroyed by the averaging process and that the process is fully reversible. They also conserve the higher moment variables to a very high degree.

The modified "box" method used by Kurihara, et al. (1979), assures conservation of the first-moment variables (e.g., mass and momentum) across the mesh interface. According to the original box method of Kurihara and Holloway (1967), the flux divergence of any quantity from a given mesh box is calculated from the sum of fluxes across the interfaces between that box and contiguous boxes. The "modified box" method consists, in part, of linearly interpolating values across an interface instead of averaging them in order to reduce interfacial noise. Conservation is assured at the mesh interface by forcing the sum of the fluxes during step 1 of the interface separation technique to exactly equal the sum of the fluxes during step 2 (Figure 8), as implied by (20a) and (20b).

Jones (1977a) pointed out that the mass flux computed across the mesh interface in the box method is sensitive to slight numerical errors, because data from two different grids with slightly different solutions must be used. Zhang, et al. (1986), also noted that a conservative interface condition like the box method is extremely complicated on a staggered grid because of the irregularly shaped boxes at the mesh interface. It is for these reasons that most modelers have avoided

the conservation condition, instead opting for a simpler interface condition that produces smooth solutions at the expense of exact conservation.

A wide range of interpolation formulae have been used to obtain the FMG interface values from the surrounding CMG grid points (Table 4). Blechman (1980) found that an overlapping quadratic Lagrangian interpolation gave better fits than a linear interpolation because of the inability of the latter to maintain continuous second derivatives (thus, over-smoothing the CMG data). Clark and Farley (1984) developed a unique quadratic formula employing a variational constraint that guarantees the conservation relation discussed above. However, a Lagrangian type interpolation appears to be the most common type of interpolation.

In contrast, various types of averaging methods for updating the CMG interface condition from the surrounding FMG grid points have been used (Table 4). Direct replacement of CMG grid point values with coincident FMG values is the simplest but least desirable approach, as the exceptionally noisy forecast fields displayed by Birchfield (1960) reveal. Since those early experiments, some kind of smoothing or averaging has been used to update CMG interface values. The only exception to this rule is the occasional use of interpolation methods in the case of complicated staggered grids (Phillips and Shukla, 1973; Phillips, 1979; Blechman, 1980).

Noise Control

Noise is always generated at the mesh interface, since there is an abrupt change in grid size and time step. This noise generally takes the form of wave reflection, as discussed earlier. According to Jones (1977b), scattering and interference of waves will cause significant noise when the disturbance on the CMG is poorly represented. External wave reflection is usually minor, since these waves are typically controlled by a damping time-integration scheme (e.g., Euler-backward method). However, internal wave motions may persist, since waves advected from the FMG to the CMG can be reflected at the nest interface, resulting in short-wavelength noise patterns across the FMG. Jones (1977b) found that advected waves with wavelengths $\lambda < 6\Delta x_c$ are totally reflected upon reaching the interface. The reflection of both gravity and advective waves at the interface can be considered to be a product of overspecification of the interface condition.

Five methods of noise control have been used in two-way nested grid models (Table 4): smoothing operators, enhanced explicit diffusion, interface conditions modified to remove overspecification, damping time-integration schemes, and mesh separation schemes. The smoothing and diffusion operators outlined earlier (Table 2) can be applied in both one- and two-way nested grid models. Jones (1977b) mentions that interface conditions modified in such a way as to remove the overspecification problem are both very difficult to employ and not totally precise in three-dimensional models. Therefore, this method

of noise control has not been widely used and will not be discussed here.

Jones (1977b) used a smoothing operator developed by Olinger, et al. (1970) near the interface to control noise and found it to be a very effective strategy. Best results were found when he smoothed a large number of points near the boundary with a weak filter. Forecast fields obtained with no interface smoothing were totally contaminated by noise (Figure 9a), whereas those obtained by using a strong filter on the 2 rows and columns closest to the interface were much improved (Figure 9b). Further reduction in noise was accomplished by using a less harsh filter (Figure 9c) and by

calculating advection at the interface using upstream differencing instead of centered differencing (Figure 9d). It should be recalled that the use of a *gradually* increasing viscosity coefficient in one-way nested models has been found to produce the most satisfactory results. Thus, it would appear that no matter whether enhanced viscosity or filtering is applied near the interface to control noise, they should not be applied abruptly. This is not to say, however, that it makes little difference whether filters or diffusive operators are used, since some filters can be very selective about which wavelengths are filtered out of the fields.

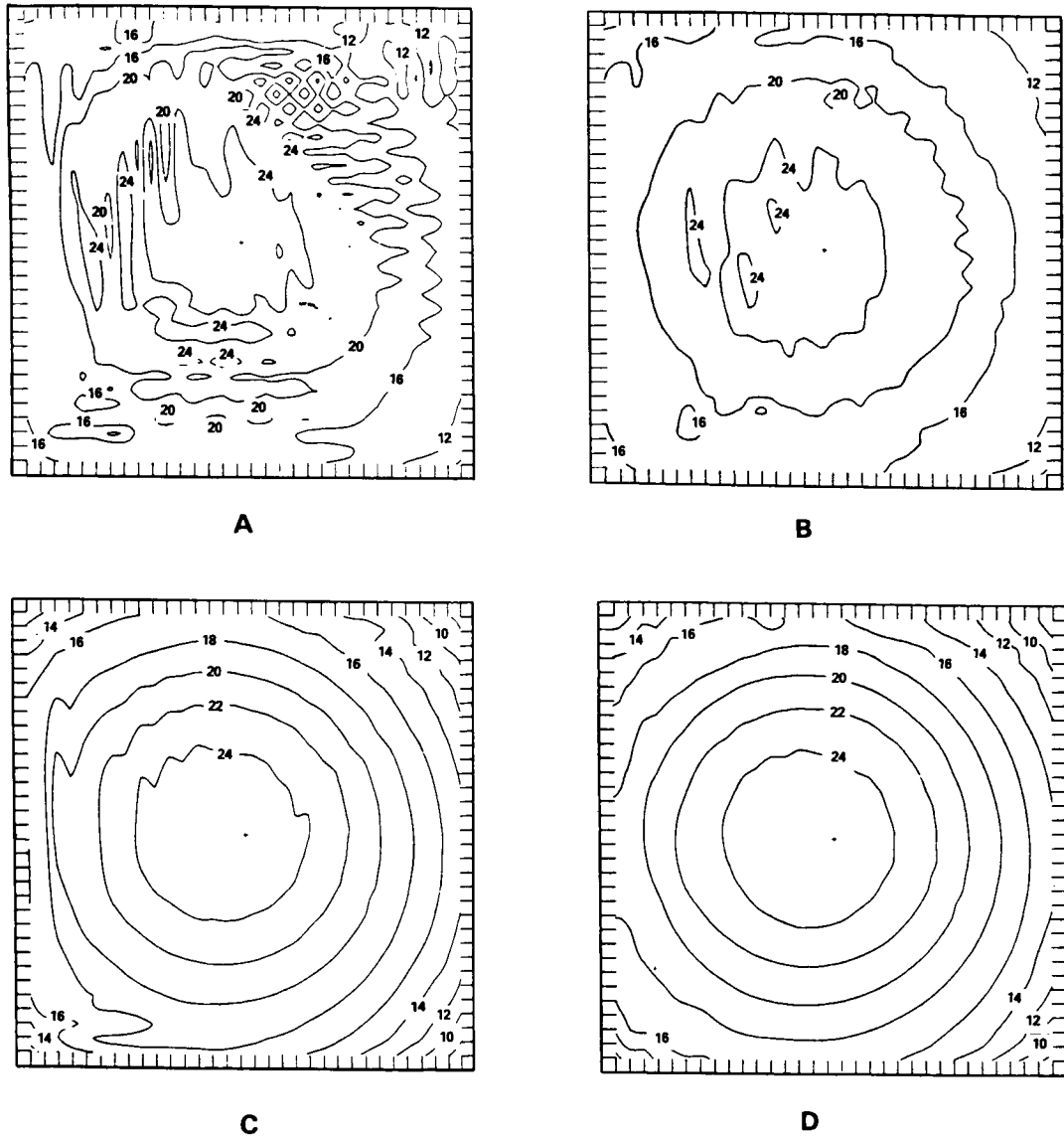


Figure 9. Mid-tropospheric vorticity fields (10^{-5} s^{-1}) associated with an analytically initialized tropical cyclone as forecast by a three-dimensional, two-way nested grid model (Jones, 1977b). Noise controlled by (a) no smoothing, (b) strong smoothing at two grid points closest to interface, (c) weaker smoothing but at six grid points closest to interface, (d) as in (c) but with upstream differencing at interface for winds at outflow points.

Tests with different degrees of viscous dissipation in two-way nested grid models have been performed by Kurihara, et al. (1979). These tests were performed with both linear and nonlinear viscosity formulations in a one-dimensional shallow water wave model to see whether a wave train would propagate freely from the CMG domain into the FMG domain (grid ratio of 2:1) and out again to the CMG domain without causing any significant noise when viscous diffusion terms were added to the wave equations. Such a test was needed because the diffusion coefficient K varies according to some power of the grid increment in either formulation. The results (Figure 10a,b) show that both linear and nonlinear viscosities reduced the amplitude of these well-resolved waves ($\lambda = 10\Delta x_c$) in the channel from their original geopotential value of $1000 \text{ m}^2\text{s}^{-2}$, but no noise was generated at the mesh interfaces. The authors also noted that

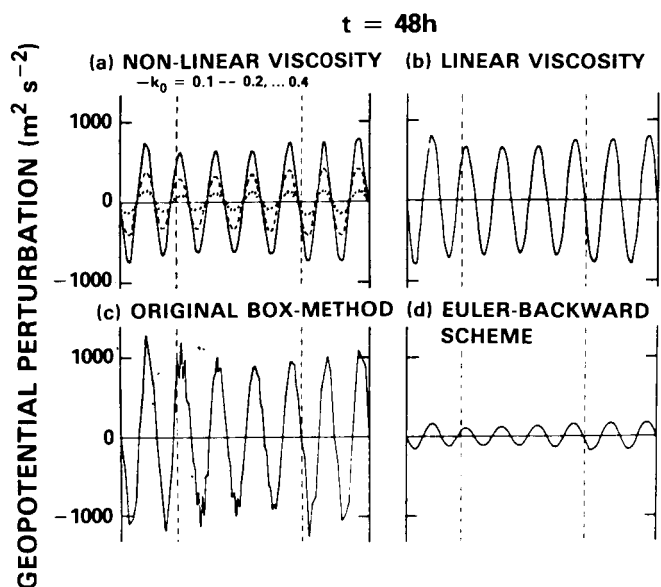


Figure 10. Forecasts at 48h of a train of 600 km waves in a two-way nested grid model with (a) nonlinear viscosity (proportional to value of k_0 shown) and (b) linear viscosity. Results of integration without viscosity by both (c) the original "Box" method and (d) the Euler-backward scheme are also shown. Dashed lines denote the mesh boundary (Kurihara, et al., 1979).

results using the "modified box-method" discussed earlier were improved over those using the original method (Figure 10c). The modified Euler-backward time integration method did a poorer job of preserving the amplitudes of these long wavelength features than did results from the original scheme (Figure 10d).

The 600 km wave train in Figure 10 was adequately resolved by the CMG so that little reflection was noticed. The model was also run for a case where the waves would not be properly resolved by the CMG. The results using a

300 km ($5\Delta x_c$) wave train (Figure 11b) show that for waves resolved in the CMG by less than six grid points, irregularities in the predicted fields became unmanageable, especially in the FMG domain, as the waves are reflected at the interface back into the domain. The addition of nonlinear viscosity does produce smoother solutions (Figure 11c), but the wave amplitude is significantly damped throughout the entire FMG domain (where it is sufficiently resolved). The effect of using a damping time integration method (the Euler-backward method) for noise control is also seen to overdamp the solution even without including viscosity (Figure 11d). Although Kurihara, et al. (1979), claimed that these tests indicate that effective noise control can be achieved in their nesting scheme by including viscous and time-damping schemes, we suggest their results may have yielded more accurate solutions had they employed increased viscosity only near the mesh interfaces where noise was being generated. Our suggested approach should preserve the amplitude of the $10\Delta x_f$ wave train in the interior of the FMG, and simultaneously remove the destructive effects of wave reflection caused by the inability of the CMG to resolve this wave train.

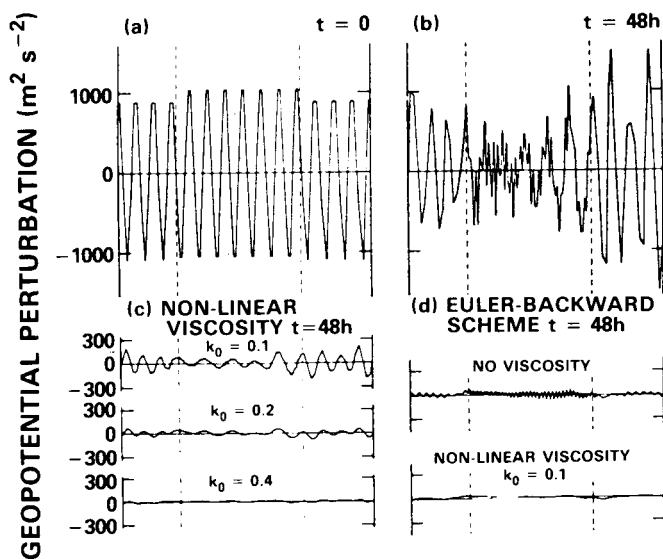


Figure 11. Integration of a train of 300 km waves in a two-way nested grid model. Geopotential fields are shown at (a) $t = 0$, (b) $t = 48\text{h}$, obtained without viscosity, (c) $t = 48\text{h}$, with viscosity and (d) $t = 48\text{h}$, computed by the Euler-backward scheme. Dashed lines denote nested mesh boundary (Kurihara, et al., 1979).

Table 4 shows that a Newtonian-type damping scheme was added to the momentum equations near the interface by Zhang, et al. (1986). Kurihara and Bender (1980) had used a similar scheme at the outer lateral boundaries of the CMG in their model. The Newtonian-type damping effect is represented in the equation of motion by a term of the form

$$\frac{\partial \vec{V}}{\partial t} = \dots (\vec{V} - \vec{V}_r) / t_d \quad (21)$$

where V_r is a reference wind value obtained from some average of surrounding wind values at the latest time level, and t_d is the relaxation time, which varied from $20 \Delta t$ at the top of the model to $100 \Delta t$ at the lowest model layer.

Most of the earlier models reviewed (Table 4) only used a combination of diffusion throughout both the FMG and the CMG domains and some form of a damping time integration scheme periodically during model simulation to help control noise (Harrison and Elsberry, 1972; Harrison, 1973; Elsberry and Ley, 1976). Later models included some type of (a) smoothing function, either throughout the entire FMG (Phillips, 1979) or just at the interface (Jones, 1977a,b), or (b) enhanced diffusion over the FMG (Kurihara, et al., 1979; Kurihara and Bender, 1980) to better control the noise. Finally, the method of noise control already mentioned in Section 4.1, namely, the separation of the input interface from the feedback interface, has been found by Zhang, et al. (1986), to also significantly reduce noise.

General Model Characteristics

Most of these models, as well as those which used one-way nested grids (Table 3) have used grid ratios $\Delta x_c / \Delta x_f \leq 4$ (Table 4). One reason for this is that higher grid ratios require too many FMG points to adequately resolve the CMG waves. Moreover, aliasing problems arise, and interfacial noise becomes unacceptably large.

General characteristics of a number of hydrostatic, two-way nested grid models are listed in Table 5. Most models, particularly those since 1976, have used the flux form of the primitive equations because of its conservative properties. Also, nearly all of these nested grid models employed a damping type of time integration scheme, such as the Euler-backward or Lax-Wendroff method. In fact, even those models which used the leapfrog scheme (which is not amplitude damping) also utilized the Euler-backward scheme periodically as a means of noise control (Table 4).

In contrast to the nearly universal use of the conservative flux form of the primitive equations during the past decade, only Kurihara, et al. (1979) and Kurihara and Bender (1980) have stressed the importance of maintaining conservation in the space differencing formulae, which is achievable with the box method. Use of a nonstaggered grid greatly simplifies its application. Models that use staggered grids require more complex interface conditions, since the mass and momentum variables must be interpolated separately. Nevertheless, a staggered grid gives more accurate solutions over the whole model domain because of reduced truncation error. Of course, errors generated by the boundary conditions at the nest interface generally exceed the truncation errors.

Many of the *two-way* interactive nested grid models initialized with *real data* (observations) have been developed

for tropical cyclone studies (Table 6). It is for this reason that only the extratropical models of Phillips (1979) and Zhang, et al. (1986) have included terrain effects (Table 5). In fact, only Zhang, et al. (1986) developed a strategy for assuring that terrain data between the FMG and CMG in the separated region (Figure 8) are made compatible. This is accomplished by requiring that the final adjusted CMG and FMG terrain values be identical at coincident points in the overlap region, and that CMG and FMG terrain values in the overlap be consistent with the interface condition filter. The results of these experiments revealed that use of compatible terrain conditions was indispensable in obtaining noise-free simulations of a jet streak as it passed over the Rocky Mountains, particularly when the interface was placed over the mountains.

A majority of the nested grid models in Table 5 considered some type of diabatic (convective or radiative) effects without adversely affecting their results. Jones (1977a) stated that cumulus parameterization schemes which depend upon calculations of the moisture/mass convergence would be error-prone near the nest interface. However, *it would appear that two-way interactive nesting is highly preferred to one-way nesting whenever strong diabatic effects are present near the interface, as suggested by Zhang, et al. (1986).*

NESTED GRID INITIALIZATION

Table 6 presents a summary of the various methods of analyzing and initializing the FMG and CMG model domains in both one- and two-way nested grid models. For the purpose of this comparison, only those models initialized with observational data are presented. Compatibility between the CMG and FMG analyses is not as important for one-way nested grid models as it is for two-way models, since the two grids are run independently in one-way simulations. This is apparently the reason that, as Table 6 shows, most one-way schemes first analyze an FMG which covers the whole CMG domain using real data and then read off the CMG data directly from the FMG analysis with no averaging. The single exception to this rule is the NASA/Langley version of the MASS model, in which the observed data are first analyzed over the CMG and then interpolated to the FMG. Harrison and Elsberry (1972) point out that, in the absence of observational data on the scale of the FMG, neither method will add any small-scale detail to the initial fields; such detail can develop only from forcing by the resolvable scales of motion or from parameterized sub-grid scale effects.

Following these separate model analysis strategies, several alternatives exist for initializing the model field analyses. One option is to use the analyses without any further modification. Alternatively, dynamical balancing between the mass and momentum fields may be imposed upon the initial grid point data analyzed on the CMG and/or FMG. Finally, some type of interpolation formula and possibly smoothing may also be utilized without regard for dynamical balancing.

TABLE 6. Method of initialization used in various nested grid models employing the primitive equations on real data.

Reference	Forecast Period (hr.)	Meteorological Application	Method of Initialization ⁽¹⁾	
			FMG	CMG
<u>One-Way Nested Grid Models</u>				
Williamson and Browning (1974)	48	Hemispheric Circulation	OA/I	Similar OA/I
Miyakoda and Rosati (1977)	48	Baroclinic Wave	OA	Read from 10-day FMG forecast over CMG domain
Leslie, et al. (1981)	24	Baroclinic Wave	OA (mass)/ BAL (momentum)	Read from FMG analysis over CMG domain
Baumhefner and Perkey (1982)	48	Baroclinic Wave	SA (mass)/GEO (momentum)	Read from FMG analysis over CMG domain
Kaplan, et al. (1983)	6	Mesoscale convection	Cubic spline INT	OA/I
<u>Two-Way Nested Grid Models</u>				
Birchfield (1960)	48	Hurricane	INT	SA
Mathur (1974)	96	Hurricane	SA of DATA*/BAL (mass)/ QG	Read from FMG analysis over CMG domain
Elsberry and Ley (1976), Ley and Elsberry (1976)	48	Tropical cyclone	SA (momentum)/ RT/BAL (mass)	
Phillips (1981)	48	Hemispheric circulation	Bilinear INT	Hemispheric Hough analysis to obtain NDV/BAL (mass)
Harrison (1981)	48	Tropical cyclone	Cubic Lagrange INT/ Analytic circulation imposed/BAL (mass)	OA
Zhang, et al. (1986)	12	Mesoscale convection, jet streak	Cubic spline INT/ Data* over FMG*	OA/I (or BAL)/ Smoothed FMG* values used in overlap region ⁽²⁾

Footnotes:

(1) Symbols used in table defined as: OA/I = objective analysis/static initialization procedure applied to data, SA = subjective analysis of data, BAL = some form of balance equation used to derive mass from momentum (or vice versa), INT = interpolation from CMG to FMG mesh, RT = "reverse telescoping" procedure (see text), DATA* = conventional data enhanced with mesoscale or other auxiliary data, FMG* = extended FMG domain, NDV = nondivergent winds, QG = quasi-geostrophic winds.

(2) Model employs compatible terrain values for FMG and CMG in the overlap region (see text).

Harrison (1973) tested the latter two types of initialization for the FMG of a tropical cyclone model. He represented the cyclone by a circularly symmetric, nondivergent vortex. His dynamical initialization employed the nonlinear balance equation to derive heights from the wind field following interpolation of the winds to the FMG. This dynamic initialization technique worked well. Harrison tested an alternative approach involving linear interpolation of the CMG data to the FMG without smoothing. This experiment produced unacceptable noise, so he advised against its use.

Others, including Mathur (1974), Ley and Elsberry (1976), Kurihara and Bender (1980), Harrison (1981), and Clark and Farley (1984) have used dynamical initialization techniques to ensure balanced fields on the FMG. Phillips (1979) and Zhang, et al. (1986) first ensured balanced fields on the CMG and then interpolated the data to the FMG. Zhang, et al. (1986) and collaborators at Pennsylvania State University presently enhance the interpolated FMG fields with any available data at fine spatial scales. Mathur (1974) was the first to use detailed data for nested grid model initialization,

but his approach of subjectively analyzing fine-scale fields over the entire CMG domain is clearly impractical and unnecessary. Ley and Elsberry (1976) agreed, however, that inclusion of fine scale data in the initialization allows the FMG to *retain* much greater detail.

An alternative approach to that used by Mathur (1974), which does not require (but can use) fine-scale data, is the "telescoping-reverse telescoping" strategy suggested by Elsberry and Ley (1976). This approach is based on the premise that, unless data are first specified on the FMG, small imbalances are created on the FMG by initializing the interface externally from the CMG, and that the resulting noise could contaminate the forecast. Their method is an adaption of the telescoping model that originated with Hill (1968) and is outlined in Figure 12 (as applied to three grids). It consists of the following five steps:

- separate analyses of the wind field are conducted for the CMG and an extended FMG (to obtain a proper interface condition with FMG resolution, the FMG is extended by four gridpoints)
- nondivergent winds for the FMG* (MMG*) domain are calculated from the stream function solved with boundary values given by the MMG (CMG).
- the stream function is recomputed for the FMG by using CMG boundary values
- the CMG is reinitialized with a nondivergent wind field computed from a Poisson equation that uses the recomputed FMG stream function for its boundary values
- the mass field is determined from the nondivergent wind field by using the nonlinear balance equation.

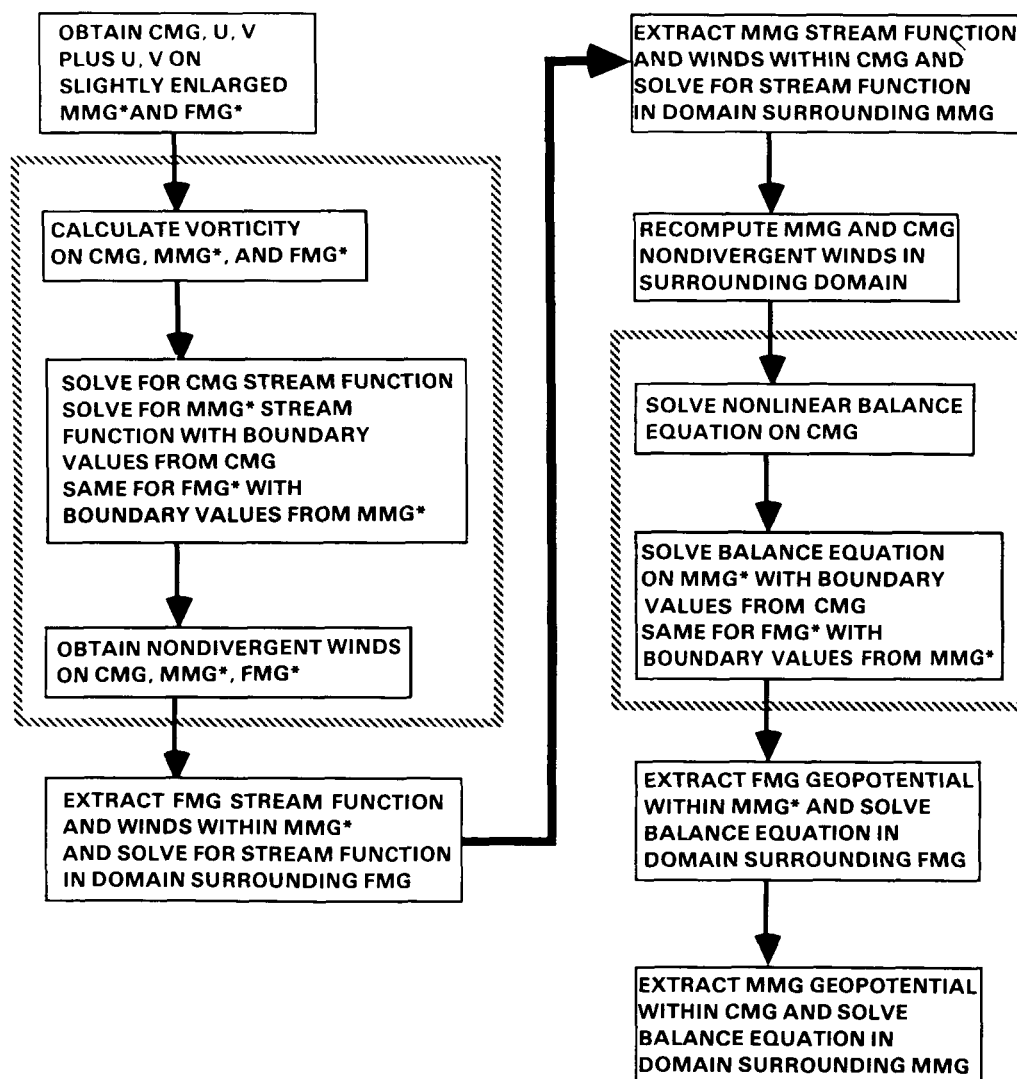


Figure 12. The telescoping-reverse telescoping strategy for initializing a two-way interaction, nested-grid model as described in the text. MMG* (FMG*) represent the slightly enlarged version of the nested medium (fine) mesh grids used during the initialization phase only. Dashed boxes enclose the steps which would correspond to a telescoping approach alone (Elsberry and Ley, 1976).

This technique forces the interface values to be part of the interior solution on an enlarged FMG grid, effectively bringing them close to dynamic balance with the FMG solution without having to conduct a fine grid initialization everywhere. Zhang, et al. (1986) used a similar technique to obtain extended FMG fields within the separated mesh grid region (A_2 in Figure 8). The nine-point Shapiro filter used for the CMG interface condition (Table 4) was also employed in region A_2 to obtain coincident CMG point values within this region. Use of this technique resulted in excellent compatibility between the initial fields on the two different meshes.

SUMMARY AND RECOMMENDATIONS FOR EXPERIMENTS

A survey of one- and two-way interactive nested grid schemes used in numerical weather prediction models has been accomplished in this report. The results of the survey can be used to make recommendations for which schemes have the greatest potential for testing with the MASS model (Kaplan, et al., 1982). The one-way approach, although it is simpler to encode on a computer, does not allow information from the fine mesh grid (FMG) to feed back to the coarse mesh grid (CMG). In a two-way nesting system, on the contrary, the predictions for both the FMG and CMG proceed simultaneously so that information is continuously exchanged between the two grids. Boundary conditions specified at the interface between the two grids permit the CMG to affect the FMG through temporal and spatial interpolations of the CMG prognostic variables (or their tendencies), and further permit the FMG to feed back to the CMG by replacing coincident CMG grid point values at the interface with those averaged from the FMG fields. The two-way strategy may be superior in cases where a small-scale atmospheric phenomenon can be expected to impact significantly on its larger-scale environment (as in the cases of mesoscale convective system, or the interaction of a jet streak with topography or boundary layer sensible heating).

One-way Interactive Schemes

Our review of one-way nested grid techniques indicated that two schemes which are stable and minimize short-wave noise created at the boundary are the sponge blending scheme (Perkey and Kreitzberg, 1976) and the radiative boundary scheme (Orlanski, 1976). The flow relaxation scheme of Davies (1983) and Leslie, et al. (1981) may also merit testing in the MASS model, although it has not been applied to general flow situations. The advective extrapolation scheme (Williamson and Browning, 1974) does not merit testing with the MASS model because of its inherent instability. The sponge blending method in the form developed by Perkey and Kreitzberg (1976) will be coded into the MASS model.

A low-pass filter that only dampens the shorter wavelength noise will be tested against the use of gradually increased horizontal diffusion near the boundary. The sponge (filter or diffusion) will be applied only after the blending of FMG and CMG tendencies has been accomplished, so as to gain maximum sponge effectiveness; furthermore, it will be applied every FMG time step.

The forward upstream difference form of the radiation boundary condition suggested by Miller and Thorpe (1981) should be tested with Carpenter's (1982) modification, which allows for blending with the CMG fields. Accordingly, the modified wave equation (19) should be used to account for a difference in phase velocity resulting from differences in grid sizes between the two meshes. A map scale factor such as the one used by Miyakoda and Rosati (1977) should also be included in the radiation scheme. Finally, a smoothing function may be tried near the boundary. Potential problems related to use of the radiative scheme at a nested grid interface where diabatic or strong orographic effects are occurring need to be evaluated in the MASS model experiments. The hydrostatic adjustment strategy developed by Miyakoda and Rosati (1977) to account for topography should also be considered. Implementation of a radiation scheme could prove difficult, however, because of the use of the Euler-backward time marching scheme in the MASS model.

Two-way Interactive Schemes

Our review of two-way nested grid schemes showed that the mesh separation structures developed by Kurihara, et al. (1979), Kurihara and Bender, (1980), and Zhang, et al. (1986), were effective in reducing overspecification error at the nest interface, thus producing smooth, relatively noise-free solutions. We intend to evaluate these mesh strategies in the MASS model. On the other hand, we will not test the technique of totally overlapping the FMG and CMG domains and yet not permitting CMG input to the entire FMG domain, (Jones 1977a,b). Schemes that conserve mass, momentum, and energy across the interface (such as Kurihara's "box" method) will also not be tested because of their complexity and the fact that most investigators have found the conservation condition unnecessary in a hydrostatic model. We will examine the utility of an overlapping quadratic Lagrange (or, equivalently, cubic-spline) method of interpolation for the FMG interface conditions. In addition, several different filters (averaging operators) will be tested for their utility as CMG interface conditions. Linear interpolation formulae and, for the CMG specifications, direct replacement of CMG grid point values with coincident FMG values will be avoided due to their undesirable side effects. The recommendations made by Jones (1977b) concerning noise control at the interface will be considered in our nesting experiments. Specifically, we will use a smoothing operator at a relatively large number of points, together with weak

filtering near the interface. The relative effectiveness of filtering compared with enhanced horizontal diffusion near the interface will be examined.

The desirability of having compatible terrain and initial conditions between the CMG and FMG in the model should also be evaluated for both one- and two-way nested grid schemes. Simulations with surface diabatic effects included near the interface will also be run in order to judge each scheme's performance when such conditions are present.

Design of MASS Nesting Scheme Experiments

The experimental design for the simulations will be like that used by Seaman, et al. (1985) in their nesting experiments, in that for each nested grid scheme to be tested:

- 1) a coarse-mesh simulation will be run over the entire model domain,
- 2) an extended fine-mesh simulation will be run over the entire model domain, and
- 3) a fine-grid simulation will be run over a subdomain nested within the larger domain.

The second experiment, which is a departure from Seaman's design, will be the control experiment from which the performance of each nested grid technique will be evaluated. The coarse-mesh model run will help provide a benchmark for demonstrating any possible improvement gained by using a nested grid model. Once the experiments are complete, final recommendations will be made as to which nested grid schemes proved most accurate and produced the least undesirable noise in the MASS model results.

The current version of the MASS model at NASA/Langley includes a one-way nested grid capability (Wong, et al., 1983). This particular version of the model has demonstrated limited success in handling deep convection in Florida. We will evaluate the performance of this scheme relative to some of the other schemes described in this report. Currently, the MASS nested grid model employs a sponge-type boundary condition; however, significant wave reflection might occur because no blending is performed at the interface (Davies, 1983). Instead, coarse-grid variable tendencies completely determine the boundary and adjacent FMG grid point (B and B-1) values. At the next two inward grid points (B-2 and B-3), the coefficient of horizontal diffusion is abruptly increased to six times the interior value ($1 \times 10^5 \text{ m}^2 \text{ s}^{-1}$), which is another possible source of interfacial noise. Cubic spline interpolation is used on the coarse grid tendencies to update the values at the boundary points of the fine grid model. However, since the boundary values are only updated every 60 CMG time steps, poor wave resolution and possible aliasing problems could arise. Other characteristics of the MASS nested model are summarized in Table 3. Appreciable short-wave noise developed in some of the results presented by Wong, et al. (1983), and the model

forecasts were terminated after 6 hours of integration. These problems likely arose because of the abrupt and simple diffusion formulation method, inadequate frequency of updating the nest interface values, and because the CMG and FMG tendencies were not blended.

The two-dimensional version of the MASS model will be employed in these nesting tests, both because of the vastly reduced computational expenses and the possibility of easily incorporating an analytically specified initial state whose time-dependent solutions are well known from theory. One such state is the finite-amplitude extension of the Eady (1949) wave model of baroclinic instability, whose semi-geostrophic solution has been derived analytically by Hoskins and Bretherton (1972). Two-dimensional, Boussinesq solutions to the Eady problem have been obtained numerically with the aid of primitive equation models in the inviscid case by Williams (1976), and with various formulations of surface friction and vertical turbulent mixing of heat and momentum in the boundary layer by Keyser and Anthes (1982) and others. In all of these studies, a cold or occluded front forms as the result of a frontogenetical process whereby shearing deformation acts upon the temperature field. The well-known aspects of both the analytical and numerical solutions permits relatively easy initialization of the MASS model fields over both the FMG and CMG domains without introducing dynamical incompatibility. Furthermore, it allows testing of various nested grid schemes within a baroclinic environment similar in structure to that which actually occurs in the extratropical atmosphere for which the MASS model was designed. Finally, diabatic effects can be included by allowing surface sensible heat effects to occur in the MASS model planetary boundary layer parameterization scheme, and so permit testing of the various nesting schemes under harsher (and even more realistic) conditions.

An example of a 24-hour simulation of the Eady wave initialized into the MASS model with a 60-hour analytic solution (i.e., an 84-hour solution) on a uniform mesh of $\Delta x = 40 \text{ km}$ and with 32 sigma levels appears in Figure 13. Periodic lateral boundaries and upper and lower level rigid, flat lids ($\dot{\sigma} = \dot{h} = 0$ at $\sigma = 0$ and $\sigma = 1$) are used as boundary conditions for the primitive equation model. An intense potential temperature gradient has developed near the center of the domain by this time (Figure 13a). The resulting vertical motion fields (Figure 13b) show a strong, thermally-direct, transverse circulation with maximum upward motions of greater than 18 mb hr^{-1} above the surface front. MASS has correctly predicted frontogenesis, compared with the analytic results at 84 hours (not shown). This simulation will act as the CMG dry adiabatic control case (experiment 1) and will be used in conjunction with the FMG control run when verifying simulations with one- and two-way nested grids. The FMG will have four times the resolution of the CMG ($\Delta x_f = 10 \text{ km}$).

Diagnostic plots of model noise can be used to quickly judge the effectiveness of different nested grid techniques.

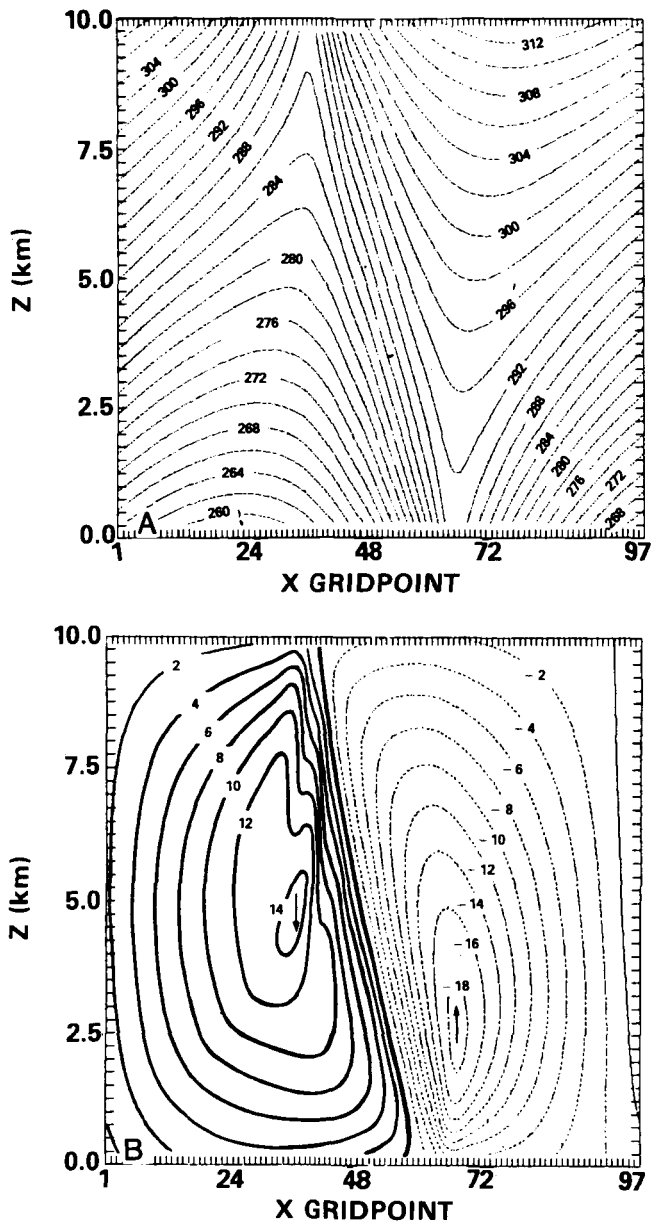


Figure 13. Results from a 24 hr. integration of the two-dimensional version of the dry, adiabatic MASS model initialized with an analytic Eady wave solution at $t = 60\text{h}$ using $\Delta x = 40\text{ km}$ and $\Delta t = 60\text{ s}$. Shown are (a) potential temperature field (intervals of 2K), and (b) vertical velocity field (intervals of 2 mb/hr) in the $x-z$ plane. Horizontal grid domain size is 3900 km.

Plots of the logarithm of the second and first derivatives of pressure ($\Pi = P_{\text{SFC}} - P_{\text{TOP}}$) with respect to time, vertical velocity at 700 mb, and surface mass flux divergence on a space-time cross section are shown in Figure 14. These results are obtained from the forecast just described. The cross

section technique is an efficient and easy way to diagnose the development and propagation of model noise generated by the introduction of different kinds of nested grid strategies.

Frontal-scale convergence and vertical motion patterns are illustrated by the fields in Fig. 14 c-d. However, a standing external gravity wave with an amplitude of $\Pi_{\text{tt}} \cong [\log^{-1}(-6.9) - \log^{-1}(-7.8)]/2 = 5.46 \times 10^{-8} \text{ mbs}^{-2}$, corresponding to a wave in the surface pressure tendency of $\Pi_t = 2.5 \times 10^{-4} \text{ mb s}^{-1} = 0.90 \text{ mb h}^{-1}$, appears in Fig. 14a and b as the result of using a fully compressible primitive equation model to integrate the Boussinesq, Eady wave equations [Dan Keyser, personal communication]. These fields give magnitudes of background noise for the control case. It is expected that significantly higher values of model noise will be present when nesting is included into MASS and that the noise should propagate inward from the nest boundary. These diagnostic plots will therefore be used to select the nesting technique that produces the least noisy model results, thus aiding in the evaluation of the various nesting schemes to be tested in the two-dimensional version of MASS.

Finally, the most accurate one- and two-way nesting methods, as determined from the two-dimensional sensitivity tests, will be evaluated against each other for a three-dimensional simulation using observational data. Any decision as whether to use either one- or two-way nested grid approaches in the MASS model may depend on what type of atmospheric phenomenon is to be simulated. These improvements to the MASS model should permit more realistic simulations of finer scale circulations that include one- or two-way interactions with the large scale circulation.

ACKNOWLEDGEMENTS

We are grateful to Michael McCumber, Michael Reeder, Louis Uccellini, and Keith Brill for their thorough reviews of this manuscript and many useful suggestions for enhancing and clarifying the subject matter. The original version of this report was typed at ST Systems Corporation.

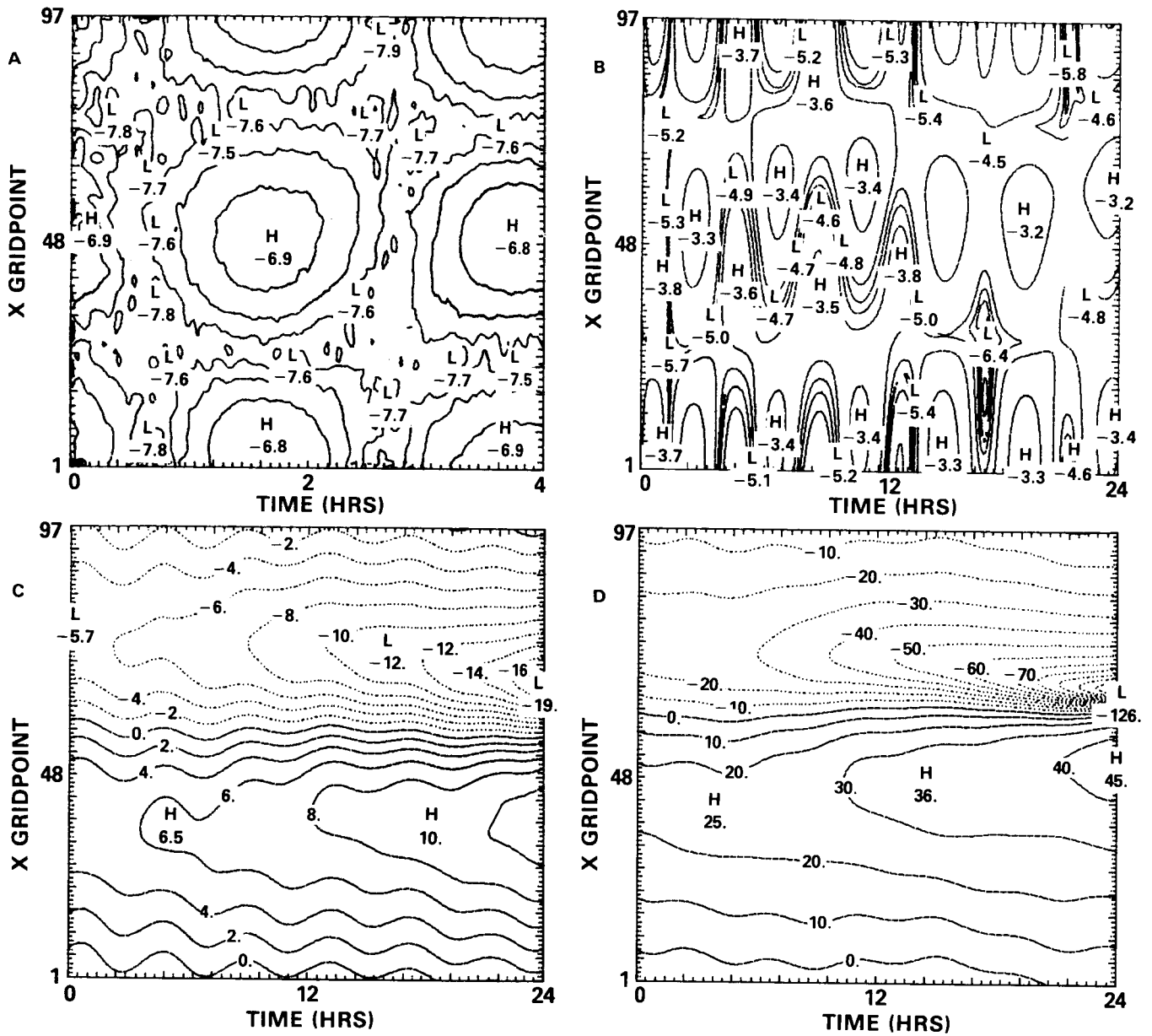


Figure 14. Results from the same model integration as Fig. 13, showing various indicators of model noise contoured on a space-time diagram: (1) $\log \partial^2 \Pi / \partial t^2$, (mb/s²), (b) $\log \partial \Pi / \partial t$, (mb/s), (c) ω (intervals of 2mb/hr) and (d) $\nabla \cdot \Pi U_s$ (intervals of 10 mb/hr), where $\Pi = P_s - P_t$. Results in (a) are for the first 4 hour of integration following smoothing, while in (b) through (d), results are shown for the full 24-hour integration with no smoothing.

BIBLIOGRAPHY

- Anthes, R.A., 1983: Regional models of the atmosphere in middle latitudes, Mon. Wea. Rev., 111, 1306-1335.
- Asselin R., 1972: Frequency filter for time integrations. Mon. Wea. Rev., 100 487-490.
- Baumhefner, D.P. and D.J. Perkey, 1982: Evaluation of lateral boundary errors in a limited-domain model. Tellus, 34, 409-428.
- Birchfield, G.E., 1960: Numerical prediction of hurricane movement with the use of a fine grid, J. Meteor., 17, 406-414.
- Blechman, J.B., 1981: Vortex generation in a nested grid numerical thunderstorm model. Mon. Wea. Rev., 109, 1061-1071.
- Carpenter, K.M., 1982: Note on the paper "Radiation conditions for the lateral boundaries of limited-area models." Quart. J.R. Met. Soc., 108, 717-719.
- Clark, T.L., and R.D. Farley, 1984: Severe downslope wind-storm calculations in two and three spatial dimensions using anelastic interactive grid nesting: A possible mechanism for gustiness. J. Atmos. Sci., 41, 329-350.
- Davies, H.C., 1976: A lateral boundary formulation for multi-level prediction models. Quart. J.R. Met. Soc., 102, 405-418.
- _____, 1983: Limitations of some common lateral boundary schemes used in regional NWP models. Mon. Wea. Rev., 111, 1003-1012.
- Eady, E.T., 1949: Long waves and cyclone waves. Tellus, 1, No. 3, 33-52.
- Elsberry, R.L. and G.W. Ley, 1976: On the strategy of initializing grid meshes in numerical weather prediction. Mon. Wea. Rev., 104, 797-799.
- Elvius, T., and A. Sundström, 1973: Computationally efficient schemes and boundary conditions for a fine-mesh barotropic model based on the shallow-water equations. Tellus, 25, 132-156.
- Harrison, E.J., Jr., 1973: Three-dimensional numerical simulations of tropical systems utilizing nested finite grids. J. Atmos. Sci., 30, 1528-1543.
- _____, 1981: Initial results from the Navy two-way interactive nested tropical cyclone model. Mon. Wea. Rev., 109, 173-177.
- _____, and R.L. Elsberry, 1972: A method for incorporating nested finite grids in the solution of systems of geophysical equations. J. Atmos. Sci., 29, 1235-1245.
- Hill, G.E., 1968: Grid telescoping in numerical weather prediction. J. Appl. Meteor., 7, 29-38.
- Hoskins, B.J. and F.P. Bretherton, 1972: Atmospheric frontogenesis models: Mathematical formulation and solution. J. Atmos. Sci., 29, 11-37.
- Jones, R.W., 1977a: A nested grid for a three-dimensional model of a tropical cyclone. J. Atmos. Sci., 34, 1528-1553.
- _____, 1977b: Noise control for a nested grid tropical cyclone model. Contrib. Atmos. Phys., 50, 393-402.
- Kaplan, M.L., J.W. Zack, V.C. Wong, and J.J. Tuccillo, 1982: Initial results from a mesoscale atmospheric simulation system and comparisons with the AVE-SESAME I data set. Mon. Wea. Rev., 110, 1564-1590.
- _____, J.W. Zack, V.C. Wong, and G.D. Coats, 1983: A nested-grid mesoscale numerical weather prediction model modified for Space Shuttle operational requirements. 9th Conf. on Aerospace and Aeronautical meteorology. Omaha, Amer. Meteor. Soc., 341-347.
- Keyser, D. and R.A. Anthes, 1982: The influence of planetary boundary layer physics on frontal structure in the Hoskins-Bretherton horizontal shear model. J. Atmos. Sci., 39, 1783-1802.
- Kurihara, Y. and J.L. Holloway, Jr., 1967: Numerical integrations of the 9-level global primitive equations model formulated by the box method. Mon. Wea. Rev., 95, 509-530.
- _____, G.J. Tripoli, and M.A. Bender, 1979: Design of a movable nested-mesh primitive equation model. Mon. Wea. Rev., 107, 239-249.
- _____, and M.A. Bender, 1980: Use of a movable nested-mesh model for tracking a small vortex. Mon. Wea. Rev., 108, 1792-1809.
- Leslie, L.M., G.A. Miles, and D.J. Gauntlett, 1981: The impact of FGGE data coverage and improved numerical techniques in numerical weather prediction in the Australian region. Quart. J.R. Met. Soc., 107, 627-642.
- Ley, G.W. and R.L. Elsberry, 1976: Forecasts of Typhoon Irma using a nested-grid model. Mon. Wea. Rev., 104, 1154-1161.
- Mathur, M.B., 1974: A multiple grid primitive equation model to simulate the development of an asymmetric hurricane (Isbell, 1964). J. Atmos. Sci., 31, 371-393.
- Matsuno, T., 1966: False reflection of waves at the boundary due to the use of finite differences. J. Meteor. Soc. Japan, 11, 145-157.
- Miller, M.J., and A.J. Thorpe, 1981: Radiation conditions for the lateral boundaries of limited-area model. Quart. J.R. Met. Soc., 107, 615-628.
- Miyakoda, K. and A. Rosati, 1977: One-way nested grid models: The interface conditions and the numerical accuracy. Mon. Wea. Rev., 105, 1072-1107.

Olinger, J.E., R.W. Welck, A. Kasahara, and W.M. Washington, 1970: Description of NCAR global circulation model National Center for Atmospheric Research, Boulder, Co, 94 pp.

_____, and A. Sundstrom, 1978: Theoretical and practical aspects of some initial boundary value problems in fluid dynamics. SIAM J. Appl. Math., 35, 419-446.

Ookochi, Y. 1972: A computational scheme for the nesting fine mesh in the primitive equation model. J. Met. Soc. Japan, 50, 37-47.

Orlanski, I., 1976: A simple boundary condition for unbounded hyperbolic flows. J. Comput. Phys., 21, 251-269.

Perkey, D.J. and C.W. Kreitzberg, 1976: A time dependent lateral boundary scheme for limited area primitive equation models. Mon. Wea. Rev., 104, 744-755.

Phillips, N.A., 1979: The nested grid model. NOAA Tech. Rep. NWS 22, National Meteorological Center, Silver Spring, MD, April 1979, 80 pp.

_____, and J. Shukla, 1973: On the strategy of combining coarse and fine grid meshes in numerical weather prediction. J. Appl. Meteor., 12, 763-770.

Pielke, R.A., 1985: Mesoscale Numerical Modeling, Advances in Geophysics, Vol. 23, 361-368.

Raymond, W. H., and A. Garder, 1976: Selective damping in a Galerkin method for solving wave problems with variable grids. Mon. Wea. Rev., 104, 1583-1590.

Seaman, N.L., H.R. Chang, D.R. Stauffer, and T.T. Warner, 1985: Simulations of mesoscale meteorology with a nested-grid numerical prediction model, 7th Conference on Numerical Weather Prediction, Montreal, Amer. Meteor. Soc., 251-258.

Sommerfeld, A., 1964: Lectures on theoretical physics, Vol. VI, No. 28, Academic Press.

Sundström, A., and T. Elvius, 1979: Computational problems related to limited-area modelling, in Numerical Methods used in Atmospheric Models, Vol. 11, Chap. 7, GARP Series No. 17, 381-416.

Williams, R.T., 1967: Atmospheric frontogenesis: A numerical experiment. J. Atmos. Sci., 24, 627-641.

Williamson, D.L., and G.L. Browning, 1974: Formulation of the lateral boundary condition for the NCAR limited-area model. J. Appl. Meteor., 12, 763-770.

Wong, V.C., J.W. Zack, M.L. Kaplan, and G.D. Coats, 1983: A nested-grid limited-area model for short term weather forecasting. Sixth Conf. on Numerical Weather Prediction, Omaha, Amer. Meteor. Soc., 9-15.

Zhang, Da-Lin, Hai-Ru Chang, N.L. Seaman, T.T. Warner, and J.M. Fritsch, 1986: A two-way interactive nesting procedure with variable terrain resolution. Mon. Wea. Rev., 114, 1330-1339.

BIBLIOGRAPHIC DATA SHEET

1. Report No. NASA TM 87808	2. Government Accession No.	3. Recipient's Catalog No.	
4. Title and Subtitle A SURVEY OF NESTED GRID TECHNIQUES AND THEIR POTENTIAL FOR USE WITHIN THE MASS WEATHER PREDICTION MODEL		5. Report Date February 1987	
		6. Performing Organization Code 612	
7. Author(s) Steven E. Koch and Jeffery T. McQueen*		8. Performing Organization Report No. 87B0116	
9. Performing Organization Name and Address Goddard Space Flight Center Greenbelt, Maryland 20771		10. Work Unit No.	
		11. Contract or Grant No.	
12. Sponsoring Agency Name and Address National Aeronautics and Space Administration Washington, DC 20546		13. Type of Report and Period Covered Technical Memorandum	
		14. Sponsoring Agency Code	
15. Supplementary Notes *Jeffery T. McQueen; ST Systems Corporation, Hyattsville, Maryland 20784			
16. Abstract <p>A survey of various one- and two-way interactive nested grid techniques used in hydrostatic numerical weather prediction models is presented and the advantages and disadvantages of each method are discussed. The techniques for specifying the lateral boundary conditions for each nested grid scheme are described in detail. Averaging and interpolation techniques used when applying the coarse mesh grid (CMG) and fine mesh grid (FMG) interface conditions during two-way nesting are discussed separately.</p> <p>This survey shows that errors are commonly generated at the boundary between the CMG and FMG due to boundary formulation or specification discrepancies. Methods used to control this noise include application of smoothers, enhanced diffusion, or damping-type time integration schemes to the model variables. Additionally, the choice of mesh structure significantly affects the amount of interfacial noise generated in two-way nesting schemes. Time and space differencing schemes, other general model characteristics, and different methods for initializing the FMG that will provide fields compatible with the CMG initialization are discussed also.</p> <p>The results from this survey provide the information needed to decide which one- and two-way nested grid schemes merit future testing with the Mesoscale Atmospheric Simulation System (MASS) model. An analytically specified baroclinic wave will be used to conduct systematic tests of the chosen schemes since this will allow for objective determination of the interfacial noise in the kind of meteorological setting for which MASS is designed. Sample diagnostic plots from initial tests using the analytic wave are presented to illustrate how the model-generated noise is ascertained. These plots will be used to compare the accuracy of the various nesting schemes when incorporated into the MASS model.</p>			
17. Key Words (Selected by Author(s)) Numerical weather prediction, nested grid models, mesoscale meteorology, lateral boundary conditions, MASS		18. Distribution Statement Unclassified - Unlimited Subject Category 47	
19. Security Classif. (of this report) Unclassified	20. Security Classif. (of this page) Unclassified	21. No. of Pages	22. Price*